The Role of the Ankle Plantar Flexors During Running with Different Strike Patterns

Amanda Susan Martin Sudduth

A thesis submitted in partial fulfillment of the
requirements for the degree of
Master of Science in Bioengineering

University of Washington
2014

Committee:
Peter R. Cavanagh, Chair
Randal P. Ching
Buddy D. Ratner
Kat M. Steele

Program Authorized to Offer Degree: Bioengineering

University of Washington

Abstract

The Role of the Ankle Plantar Flexors During
Running with Different Strike Patterns

Amanda Susuan Martin Sudduth

Chair of the Supervisory Committee:
Peter R. Cavanagh, Professor, Vice Chair of Research
Orthopaedics and Sports Medicine

Different strike patterns result in differences in kinematics and kinetics during running. The objective of this study was to examine differences in muscle activation in rearfoot stike (RFS) and nonrearfoot strike (nRFS) running. It was hypothesized that the activation of the medial grastrocnemius would be earlier and of greater magnitude in runners using a nonrearfoot strike pattern. Furthermore, it was hypothesized that the medial gastrocnemius would show two distinct peaks in activity in nonrearfoot striking, the first resulting from preparation for, and support of, initial contact and the second from propulsion during the stance phase. Finally, it was hypothesized that the activation of the tibialis anterior would be earlier and of greater magnitude in runners using a rearfoot strike pattern. This study included 9 female runners, five habitual rearfoot strikers and four habitual nonrearfoot strikers, who each completed 3-dimensional running analysis under two conditions: their habitual strike pattern and a converted strike pattern during which habitual nonrearfoot runners converted to rearfoot and habitual rearfoot runners converted to nonrearfoot. Variables of interest were activation of the medial gastrocnemius and tibialis anterior, lower body kinematics, body segment positions and velocities at foot strike, and tibial acceleration. This study found no significant differences in the activation time or magnitude of the tibialis anterior or medial gastrocnemius muscles during RFS and nRFS running. Visual inspection of the medial gastrocnemius electromyography (EMG) data showed the hypothesized pre-foot strike activation peak in the nRFS condition, however because of the small number of subjects and high variability of the EMG data, this difference was not statistically significant and should be investigated further. Resultant tibial acceleration was greater in the nRFS condition, indicating a potential factor for increased risk of tibial stress fracture in individuals running with a nRFS pattern.

Acknowledgements

Many individuals deserve thanks for helping me over the course of this research. My advisor, Dr. Peter Cavanagh, provided countless support and guidance. No matter how busy he was, he always made time to help me work out problems and talk through ideas. I would also like to thank the members of my committee, Dr. Randal Ching, Dr. Kat Steele and Dr. Buddy Ratner. Thanks to Molly Glauberman, who helped me with subject testing and always had the answer to anything I asked her. I could not have asked for a better person to have my desk next to for two years.

I would like to thank all of my friends, who have been there for me on a daily basis and keep me sane. My boyfriend, Jake, who has supported me throughout my graduate career and never failed to make me laugh even when I was stressed out, sleep deprived or just in a bad mood. Finally, I would like to thank my parents, I would not have gotten to where I am today without you. Dad, you stayed up late helping me with physics and calculus problems in high school, dusted off your thermodynamics textbook from college when I was totally lost during that class, and still answer the phone every time I need help or have a random question. Mom, you were always happy to edit anything I wrote before I turned it in, no matter how dry the subject matter was, you never failed me when I asked for a pep talk and sent me countless pictures of our dog, Leo, to keep me entertained. Also, thank you Leo for being so cute.

Contents

List of Figures

List of Tables

Chapter 1

Introduction

Distance running continues to increase in popularity both competitively and for recreation. This growth in participation has occurred despite the high injury rates associated with distance running [20, 41, 34, 42]. Because of this, the incidence of, and potential risk factors for lower extremity running injuries have been researched in long distance runners, with studies reporting variations in injury incidence from 19% to 78% [64]. A systematic review of 17 running injury studies in long distance runners found that weekly training distance along with having sustained a previous injury were risk factors for the development of running injuries [64].

The majority of runners make first ground contact with their heels [30, 38], although a strike pattern ranging from rearfoot (heel strike) to forefoot is possible. Nonrearfoot strikers land predominately on their midfoot or forefoot before (usually) bringing their heel down to the ground. In contrast, rearfoot strikers first land on their heel and then bring their forefoot into contact.

Several prior studies have examined the biomechanical differences between different strike patterns through the study of kinetics, kinematics and muscle function. Hreljac and colleagues proposed that high repetitive vertical loading rates and large impact forces, measured using a force platform, during running lead to injury [33, 32]. Because of potential links between vertical loading and foot strike pattern, the implications of foot strike pattern in lower limb injury have gained attention. Individuals using a rearfoot/heel strike pattern have an initial impact peak during the first 50 ms of stance phase [11] which is absent in their nonrearfoot striking counterparts [69]. Nonrearfoot striking has been advocated by practitioners and some researchers because of its association with the reduction of impact forces [38], and in turn the theoretical decrease in susceptibility to injury [37].

Throughout the gait cycle, appropriate timing and magnitude of muscle activation is vital in preparing for impact, determining lower limb stiffness, and modulating joint loading [47]. Previous research has produced limited conclusions as to the variation of muscle activation and activity between different foot strike patterns. Olin and colleagues found that, when transitioning from shod to barefoot running, the average muscle activity of the medial gastrocnemius was greater in barefoot running, while the activity of the tibialis anterior was highest in shod rearfoot striking [48]. This study used foot switches placed under the heel and ball of the foot to determine when heel strike and toe strike or toe off occurred, respectively. Using the foot strike and toe off time points, all electromyography (EMG) data were

cropped from foot touch down to toe off, which eliminated any muscle pre-stance activation data and thus potential differences between conditions. EMG data were then band-pass filtered (2nd order, zero-lag Butterwoth filter, cut-off frequencies of 20 and 300 Hz), rectified and smoothed using a low-pass filter (2nd order, zero-lag Butterwoth filter, cut-off frequency of 7 Hz), and normalized to the maximal EMG activity found in all trials for each subject and each respective muscle. This study did not include shod nonrearfoot striking as a test condition, and only reported average and peak muscle activity during stance.

Significant differences between rearfoot and nonrearfoot strike patterns were also observed by Shih and colleagues in the pre-activation of the tibialis anterior and medial gastrocnemius in an all-male study [57]. In this study each subject was tested, and EMG data recorded for each target muscle for a five second long maximum voluntary contraction where resistance was applied. The maximum voluntary contraction was then used to normalize the dynamic muscle activity for each participant. When compared to their male counterparts, females have been found to be more prone to developing running related injuries, including stress fractures [4, 62]. Because of this, the differences in muscle activation time and magnitude between different strike types during shod running in a female subject population still requires further investigation. Studying these differences is key to the overall understanding of the implication of foot strike patterns on kinematics, kinetics and muscle function during running.

The present study aimed to examine the effects of strike pattern on the role of dorsi- and plantar flexors, specifically the tibialis anterior and the medial gastrocnemius, during running. The specific objective of this study was to examine muscle activation, tibial acceleration and kinematic and kinetic variables in runners using a rearfoot strike pattern versus a nonrearfoot (mid-foot or forefoot) pattern. The specific hypotheses tested are as follows:

1. Activation of the medial gastrocnemius will be earlier and of greater magnitude during nonrearfoot striking as compared to rearfoot striking.

2. Nonrearfoot striking will result in two peaks in medial gastrocnemius muscle activity, the first corresponding to preparation for, and support of, initial contact and the second corresponding to propulsion during the stance phase.

3. Rearfoot striking will result in earlier and greater magnitude activation of the tibialis anterior muscle associated with the controlled dorsiflexion needed during foot strike.

4. Nonrearfoot striking will result in a larger resultant tibial acceleration.

Chapter 2

Background

2.1 Running and injury trends

Approximately half of all runners sustain an injury annually during their chosen sport [26, 64]. Among the risk factors found for the development of running related injuries include higher weekly mileage, a history of previous injury and those who increased training miles per week [64, 40]. Stress fractures are among the most common overuse injuries associated with running [20, 42, 34], accounting for up to 20% of injuries seen in sports medicine clinics [22]. The tibia is especially prone to stress fractures, with tibial stress fractures accounting for between 35% and 56% of all stress fractures [41, 49]. Repeated loading that is undergone by the lower extremities during running increases the likelihood that an individual will develop a stress fracture [34]. Research has indicated that high vertical loading rate and magnitude may be a risk factor in the development of tibial stress fractures [44, 33, 49, 16]. It has been reported that females are more prone to running injuries, including stress fractures, as compared to their male counterparts [4, 62].

Due to the high risk of injury associated with running, various efforts have been undertaken for injury prevention. Numerous studies have looked at the implications of different foot strike patterns in injury incidence [13, 33, 51]. The majority of shod runners use a rearfoot strike (RFS) pattern in which they first make contact with the heel, and then bring down the forefoot [30, 38]. Nonrearfoot strike (nRFS) patterns involve making contact first with the midfoot or forefoot and then bringing down the heel. There has been a recent trend in using nonrearfoot strike modification in an attempt to reduce injury. Because of the observed reduction in impact forces [38, 15], some researchers [38, 12] advocate for adoption of a more forefoot strike pattern. However, a study of 341 soldiers found no difference between the injury rates of different running styles [67].

An early study [11] examined ground reaction force (GRF) and changes in the center of pressure distribution throughout the stance phase of running. Subject strike patterns were classified as forefoot, midfoot or rearfoot according to the location of the center of pressure at the time of first contact. The mid-line of the shoe was divided into thirds, and runners striking in the posterior third were classified as rearfoot, medial third as midfoot and anterior third as forefoot. Another method for the classification of foot strike pattern was developed based on the foot strike angle as measured in the sagittal plane at initial contact [2]. Foot

strike angle was defined as the angle between the vector from the heel to dorsum of the foot at the head of the third metatarsal and the anteroposterior axis of the running surface (Figure 2.1). The foot strike angle during standing was subtracted from the angle during running to define a flat foot as 0 degrees with positive angles indicating dorsiflexion. Foot strike patterns classified by foot strike angle (FSA) are outlined in Table 2.1.

Table 2.1: FSA for rearfoot, midfoot and forefoot strike patterns as defined by Altman et al.

Foot Strike Angle (deg)	
Rearfoot	FSA> 8.0
Midfoot	$-1.6 <$ FSA < 8.0
Forefoot	FSA< -1.6

2.2 Impact forces

2.2.1 Ground reaction force

Ground reaction force (GRF) is typically measured using surface mounted force plates, which measure the net force that is acting on the body's center of mass, reflecting the average acceleration of the whole body [59]. Differences in foot strike pattern result in a contrast in kinetics, especially at contact. Rearfoot strikers show a distinct initial impact peak in GRF, with high rate and magnitude during the first 50 milliseconds after foot strike [59], which is then followed by a larger peak at approximately 100-150 milliseconds into stance [11, 15]. Nonrearfoot strikers do not show an initial impact peak at foot strike, only the large peak during mid-stance similar to that of rearfoot strikers [11, 8, 38, 37, 69, 15, 23] (Figure 2.2). Despite the absence of the vertical impact peak in the GRF of those running with a nonrearfoot strike pattern, higher impact frequencies are still present, although they do not show up as a peak in the time domain [58]. During running the magnitude of the GRF increases with increasing running speed [45], and joint contact forces can reach magnitudes 8-15 times body weight [19, 53]. This suggests that GRF impact peaks may not be the best indicators for the development of running injuries, and that internal loading may be more indicative of injurious forces.

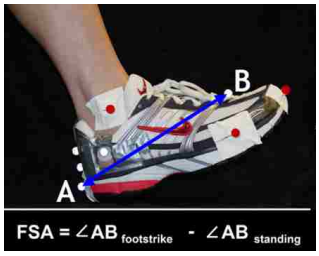

Figure 2.1: Foot strike angle as defined by Altman et al. [2]

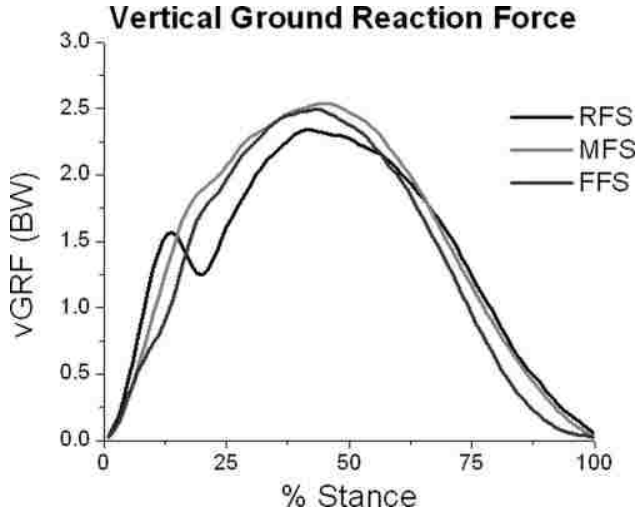

Figure 2.2: Vertical GRF during contact phase of running for forefoot, midfoot and rearfoot strike patterns [1].

2.2.2 Impact "shock"/acceleration

Impact peaks have been implicated in contributing to injury due to the shock wave that is generated and travels up the body, resulting in potentially high stresses and strains on skeletal tissue [59]. Accelerometers attached to the body by either bone pins [35, 36] or skin mounting [59, 14] have been used to measure the propagation of the impact shock wave. Skin mounted accelerometers have soft tissue between the transducer and the bone thus altering the acceleration measured compared to bone mounted sensors. These effects of soft tissue on the acceleration signal can be minimized by the use of light weight accelerometers which are preloaded with an elastic strap that is tightened up to the limit of the subject's comfort [59]. In addition to the soft tissue effects, impact shock transmission can also be influenced by the cushioning effects of footwear, as well as kinematic adaptations to impact. While studying the effect of tissue composition differences on tibial acceleration during running, researchers found that females experienced 25% greater peak acceleration than males [54], supporting the increased risk of tibial stress fractures in females. It is possible that females experience greater acceleration during impact because of differences in lean mass and bone mineral content compared to their male counterparts. In general, females have decreased lean mass and bone mineral content, which could affect the propagation of impact shock through the body and result in greater tibial accelerations due to greater shock absorption by the tibia. Increased magnitude and rate of knee flexion during contact, and different foot strike patterns may reduce impact shock during running [21, 43]. Impact shock has been determined to vary systematically with running speed and gradient [28, 59], with the frequency and amplitude of impact peaks increasing with increasing running speed [59].

In one study, individuals with a history of tibial stress fractures had an increase in instantaneous and average vertical loading rate, as well as peak tibial shock compared to a control group [44]. However, the findings of this study are limited in their application as they have not been replicated and the number of runners tested was small (40 subjects). This has caused many researchers to look into methods to decrease variables associated with high

impact during running. Some studies have found that an increase in rates and magnitudes of impact loading, seen in rearfoot strikers, correlates with injury to the lower extremities, including stress fractures [44]. However, other studies have found no correlation between impact peaks and injury rates [46].

2.3 Kinematics and kinetics of the lower extremities

As previously discussed, there is a continuum of foot strike patterns observed during running. These range from impacting the ground first on the heel/rearfoot to initial contact being made with the midfoot to those who strike the ground first with the forefoot. Approximately 75% [30] of traditionally shod runners utilize a rearfoot strike pattern when running. Rearfoot strikers impact the ground with the knee extended and the foot in front of the knee and hip, as well as the ankle dorsiflexed, and after impact the runner rapidly plantar flexes [17]. Nonrearfoot strikers have more knee flexion upon impact and the runner's ankle is plantar flexed. Contact is made on the ball of the foot, which is immediately followed by dorsiflexion of the foot during impact and an increase in ankle and knee compliance [38].

Numerous studies have compared the kinematic differences between rearfoot and nonrearfoot strike patterns [51, 38, 18, 57, 31, 48] as well as exploring the implications of these differences in injury. Individuals who run with a rearfoot strike pattern contact the ground on the heel and with the ankle dorsiflexed, while those using a nonrearfoot strike pattern range from a neutral ankle position at foot strike to a plantarflexed ankle, the result of landing on the midfoot and forefoot, respectively [3, 68]. As a result of the increase in ankle plantar flexion, ankle joint moments are greater at foot strike during nonrearfoot running compared to rearfoot running [51, 15]. Research has shown that runners utilizing a nonrearfoot strike pattern have a greater knee flexion at foot strike compared to those using a rearfoot strike pattern [48, 18, 57, 3]. The increase in knee flexion is the result of the runner's need to compensate for a more plantar flexed ankle during nonrearfoot running [57, 69]. In addition, Heiderscheit et al. found that peak knee flexion angle decreased with increasing step rate [31], which occurs during nonrearfoot running [18, 31]. In comparing running in minimalist shoes [70] and barefoot running [48] with traditional shod running, a greater knee flexion angle was seen at foot strike in minimalist and barefoot runners due to their adaptation of a more forefoot strike pattern.

It has been hypothesized that the rate and magnitude of joint moments may cause repetitive stress damage in connective and stabilizing tissues [6]. The joint moments of the lower extremities are also different depending on strike pattern. Daoud et al. have shown that nonrearfoot striking is associated with a larger net moment about the ankle in the sagittal plane compared to rearfoot striking, but a decrease in the net moments about the knee and hip in the sagittal and transverse planes [15]. This is likely the result of a shift in demand from the hip and knee in rearfoot stiking to the ankle and foot in nonrearfoot striking.

2.4 Muscle activation

Running is accomplished through the coordinated activation of a number of skeletal muscles in the lower extremities, which results in muscle contractions that facilitate movement.

Muscle contractions can be categorized as either concentric, eccentric, isometric or isotonic [56]. Concentric contractions occur when the force generated is sufficient to overcome the external load on the muscle, which allows the muscle to shorten. When the force generated is insufficient to overcome external loading on the muscle, the muscle eccentrically contracts as the result of the muscle fibers lengthening as they contract. Isometric contractions are the result of the muscle contracting without a change in fiber length. Lastly, an isotonic muscle contraction is when the tension in the muscle remains constant, despite a change in muscle length occurring. The force-length and velocity-length relationships describe the ability of muscle to generate force as a dependence on the length and velocity of the muscle fibers, seen in Figure 2.3. The force-length relationship relates the strength of an isometric contraction that a muscle is able to produce to the length of the muscle at which the contraction occurs. When muscles are at a length close to an ideal length (often their resting length), they are able to act with the greatest active force. The further the muscle is from this ideal length, the less force it is able to produce. The force-velocity relationship of muscle reveals that the speed at which muscle changes length affects the amount of force it is able to generate. These two relationships have many implication in biomechanics, including limiting an individuals running speed. Gruber et al. found implications that nonrearfoot runners may run with decreased plantar flexor force that is required to produce a given joint moment [27], and that rearfoot runners may have increased plantar flexor force while running but have optimal muscle shortening velocities.

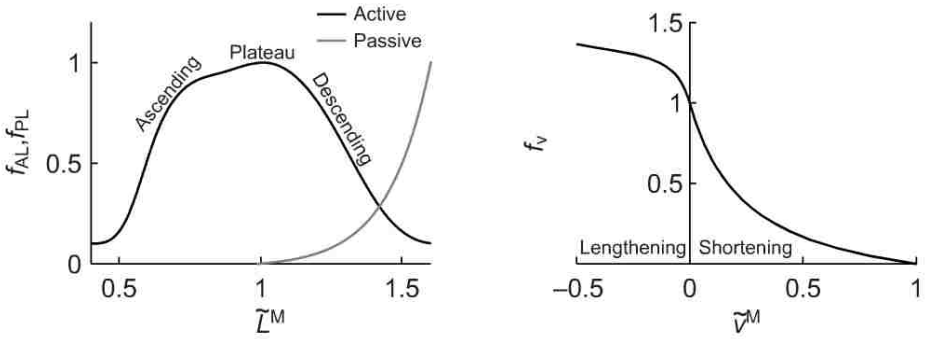

Figure 2.3: Model of the muscle force-length relationship (left): shows effects, active/passive force-length multipliers f_{AL} and f_{PL}, of normalized fiber length ($L^{\ M} = L^M/L_0^M$, with muscle fiber length, L^M), on the active and passive force generated by muscle fibers. Model of the force-velocity relationship (right): shows effect, force-velocity multiplier f_v, of normalized fiber velocity ($v^{-M} = v^M/v_{max}^M$, with fiber shortening velocity, v^M) on active force generated by muscle fibers [5].

Electromyography (EMG) is routinely used to characterize muscle activations during running. The use of EMG is limited in that it is unable to provide information as to the force a muscle is producing during motion. Futhermore, an electromechanical delay (EMD) exists between the onset of electrical activity (EMG) and the onset of mechanical response (force). The length of EMD varies depending on the type of contraction the muscle undergoes [10]. Therefore, while EMG is useful in studying the onset of electrical activity in muscle

during motion, this is not directly applicable in determining the time of onset of muscle force. Despite limitations, the use of EMG in biomechanical motion analysis provides useful data regarding the time, duration and the degree of activity that a particular muscle contributes to motion.

This study focuses on the tibialis anterior and medial gastrocnemius, and their role in plantar flexion during running with different strike types. The tibialis anterior functions concentrically to dorsiflex and invert the foot, and eccentrically to control the rate of plantarflexion of the ankle. In contrast, the medial gastrocnemius acts concentrically to plantar flex the foot, and eccentrically to control the rate of ankle dorsiflexion and accelerates the knee into extension due to dynamic coupling [55]. The tibialis anterior is activated during the pre-stance phase in rearfoot striking in order to eccentrically control the plantar flexion at the ankle needed at foot strike [18, 65, 57, 66]. The eccentric activity of the tibialis anterior can be decreased through the utilization of a nonrearfoot strike pattern [63, 61, 57, 23], which decreases the amount of dorsiflexion at the ankle. Instead, foot strike occurs while the ankle is plantar flexed. After initial contact is made during nonrearfoot striking, the ankle dorsiflexes, which is controlled through eccentric contraction of the gastrocnemius. Greater activation of the gastrocnemius during pre-stance and stance phase has been seen in runners using a nonrearfoot strike pattern as compared to those using a rearfoot strike [57, 23]. This is likely because the plantar flexors need to counteract the dorsiflexion moment that occurs when the foot strikes the ground with a midfoot or forefoot pattern. The medial gastrocnemius has also shown an increase in peak EMG activity with increasing running speed [60].

It has been proposed that impact forces are used by the body as input signals during running, which produce muscle activation shortly before the next ground contact in an effort to minimize the vibration of soft tissue and reduce the loading of joints and tendons [46]. From this, it follows that the pre-impact muscle activation would be visible in the EMG signal of those muscles of the lower extremity that are in a sense "anticipating" the impact. The current study has hypothesized that such pre-activation will be visible in the tibialis anterior in rearfoot striking as the foot is dorsiflexed in preparation for impact, and in the medial gastrocnemius in nonrearfoot striking when the muscle is activated before it is required to bear a significant amount of impact force.

2.5 Adoption of different strike patterns and the trend of barefoot running

There has been a recent trend toward minimalist footwear and even barefoot running, encouraged primarily by certain anthropological studies [38]. In one survey of runners, over 75% indicated an interest in minimalist or barefoot running [52]. The primary motivation for interest was the prevention of future injury. Because minimalist footwear does not provide the heel cushioning of traditional running shoes, a midfoot/forefoot strike pattern is frequently adopted in order to distribute the impact force over a greater area of the foot. Since transitioning to minimalist or barefoot shoes initiates the adoption of a new, more anterior foot strike pattern [25, 61], it is somewhat unclear whether observed biomechanical differ-

ences are a result of the change in footwear, foot strike pattern or a combination of both. A more forefoot strike pattern during minimalist running also allows for greater absorption of impact by the plantar flexor muscles [38, 17]. However, there is no prospective evidence that injuries are reduced by training a habitually rearfoot striking runner to run with a forefoot striking pattern in minimalist shoes. In fact, two recent studies have suggested that the opposite may occur and reported that transitioning to minimalist footwear resulted in stress injuries or fractures [24, 50].

Traditionally shod runners can also adopt a different strike pattern while wearing conventional running shoes through the alteration of their running style. There is no evidence of a difference between the internal loading of joints of habitual shod runners and those who converted their foot strike type [51]. GRFs and loading rates during impact have been compared between habitual rearfoot strikers and habitual forefoot strikers. A recent study also examined the effects of individuals switching their foot strike pattern on GRF and loading rate during running [9]. Peak impact GRFs were found to be similar for both habitually and converted runners using a rearfoot strike pattern. When habitual forefoot strikers altered their strike pattern to a rearfoot strike, they demonstrated a larger GRF impact peak when compared to converted runners using a forefoot strike pattern. Interestingly, both individuals who converted to a forefoot strike pattern and those who converted to a rearfoot strike pattern exaggerated the new strike pattern when compared to the habitual groups [9]. Additionally, strike modification toward a nonrearfoot strike has been successfully used to treat individuals suffering from anterior compartment syndrome, possibly through decreasing activity of the tibialis anterior and reducing anterior compartment pressure [61, 18].

Chapter 3

Methods

3.1 Subjects

Nine habitually shod female recreational runners ($(Mean \pm SD)$ age= 28.6 ± 3.7 yr, height= 65.9 ± 2.7 in, weight= 127.7 ± 20.8 lbs), running on average more than 25 miles per week, participated in this study. All subjects provided informed consent approved by the University of Washington's Institutional Review Board. Subjects confirmed on a screening form that they were between the ages of 18-40 years old, that they were running injury free more than 25 miles/week, that they had participated in a race in the past 12 months, and were not a barefoot or minimal shoe runner.

3.2 Instrumentation

3.2.1 Motion capture

Kinematic data were sampled at 100 Hz using an eight camera Nexus system (VICON, Oxford, UK). The infrared cameras were set up in a circle, creating a capture area surrounding the instrumented treadmill in the gait laboratory. Retro-reflective markers (VICON, Oxford, UK) attached to the subject using double sided tape (VICON, Oxford, UK), as described in Section 3.3.1, were tracked by the infrared cameras and data were collected and stored by the Nexus system.

3.2.2 Ground reaction force

Ground reaction force (GRF) data were sampled at 1000 Hz in the vertical direction using a Kistler force platform (Kistler Instrument Corp., Amherst, NY) mounted beneath a treadmill belt (Figure 3.1). GRF signals were passed through an analog to digital converter, and then collected simultaneously with motion capture data by the Nexus system.

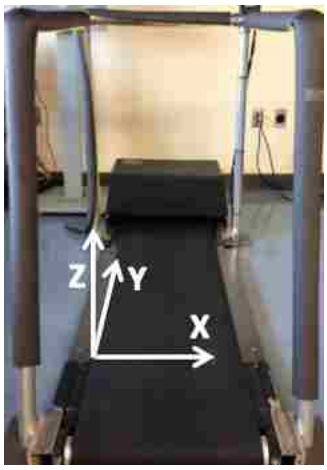

Figure 3.1: Treadmill and data collection coordinate system.

3.2.3 Tibial acceleration

An acceleration monitoring unit (ZIN Technologies, Cleveland, OH) was used to quantify tibial acceleration. The system consisted of two sensors, a tri-axial accelerometer ($\pm 12g$), a tri-axial rate gyro ($\pm 2000°/sec$) and a wireless Bluetooth transmitter. The overall dimensions of the sensor were 40 mm x 22 mm x 12 mm, with a packaged mass of 21 grams. The acceleration monitoring unit was attached to the subject's right leg, and tibial acceleration data were sampled at 512 Hz. A Bluetooth radio built into the sensor unit allowed signals to be collected on a laboratory computer via custom MATLAB (MathWorks, Natick, MA) software.

3.2.4 Electromyography

Electromyography (EMG) data were collected from the tibialis anterior and the medial gastrocnemious on the subject's right leg. A KinetiSense Biokinetic Analysis System (CleveMed, Cleveland, OH) was used to collect EMG data. The KinetiSense included two components, the command module and the motion sensors. Each motion sensor housed three accelerometers and three gyroscopes, which measured linear acceleration and angular velocity, respectively, about the x, y and z axes. The motion sensors were linked to the command module via wireless data transmission. The command module included a memory card, battery and EMG amplifiers, with a DIN connector input for two channels of EMG data. The KinetiSense command module sampled motion sensor data at 128 Hz. EMG data were sampled at 2048 Hz, with the root mean square value calculated and output at 128 Hz to allow for data synchronization between the EMG and motion sensors. One motion sensor was used in order to identify foot strike for the syncing of the EMG data with kinematic and kinetic data. This sensor was attached to the heel of the subject's right shoe using double sided tape.

3.2.5 High speed video

High speed video was collected at 300 frames/sec using a Casio EX-F1 camera (The Casio Computer Company, Ltd., Tokyo, Japan) for the last 30 seconds of each trial for each of the nine subjects. This video was used as a visual confirmation of the subjects' foot strike pattern, both naturally and after they made an attempt to switch their strike pattern. A spotlight was required in order to shoot the high-speed video, which would have interfered with VICON data collection. Because of this, high speed video was collected at the end of each trial and not simultaneously with other data collection.

3.3 Experimental protocol

Subjects reported for one testing session of approximately 60 minutes in length. Informed consent was obtained at the beginning of each session, and anatomical measurements were recorded along with the subject's age, weight and height. Each subject wore a pair of Brooks Adrenaline GTS 13 running shoes (Brooks Sports, Inc., Seattle, WA) provided by the investigator in their shoe size for the duration of testing. This insured that there were no variations in shoe cushioning, which could have affected data.

3.3.1 Subject preparation

Subjects were first outfitted with the acceleration monitoring unit placed on their right tibia for collection of tibial acceleration (Figure 3.2). To position the monitoring unit, the most prominent area of the medial malleolus on the right ankle was identified and marked with a pen. A line 5 cm superior to this point was marked on the tibia. The medial and lateral edges of the tibia were then identified through palpation, and a box was drawn in the area where the sensor was to be affixed, with the lower edge of the sensor on the 5 cm line. To eliminate slipping the area was then covered with a self-adhesive bandage. The sensor area was traced over on the bandage using a pen. The sensor was then turned on and placed in the marked area as flat against the tibia as possible. The sensor was secured to the subject's leg using a Velcro strap, which was tightened to 22 N (5 lbs) of tension using a digital hanging scale (American Weigh Scales, Inc., Norcross, GA). After the monitoring unit was secured to the subject's leg, the angle of the sensor with respect to the sagittal plane (θ) was calculated (Figure 3.3) for use in data analysis.

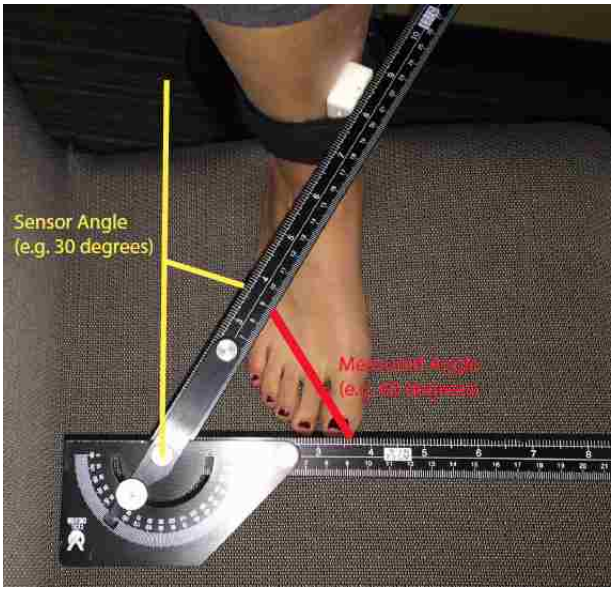

Figure 3.3: Convention for the calculation of sensor angle. The measured angle was subtracted from 90 degrees to calculate the sensor angle.

Next, the KinetiSense system was prepared for EMG data collection. Light abrasion with a fine grain sandpaper was used to prepare the area of skin before the electrodes were adhered to the leg. After the area was abraded, an alcohol wipe was used to clean off any dead skin and the skin was allowed to dry. Five disposable surface electrodes (Bio-Medical Instruments, Warren, MI) were used for the EMG data collection for each subject, two placed on the medial gastrocnemious (channel 1), two on the tibialis anterior (channel 2) and one placed on a bony prominence (superior tibia directly under the knee) to be used as a ground (Figure 3.4). On the two muscles of interest, the complementary electrodes were placed 5 cm apart and were oriented in the direction of the muscle fibers, diagonally on the medial gastrocnemious and vertically on the tibialis anterior. The EMG leads were connected to the snap electrodes as well as the KinetiSense command module. The module was clipped onto the subject's shorts and a self-adhesive bandage was wrapped around the electrodes to ensure good contact was made, as well as to secure the leads to the subject's right leg. A KinetiSense motion sensor was then attached to the heel of the right shoe adjacent to the inferior calcaneous as seen in Figure 3.5. This sensor collected acceleration data concurrently with the EMG data collection, which enabled the identification of foot strike in the EMG data.

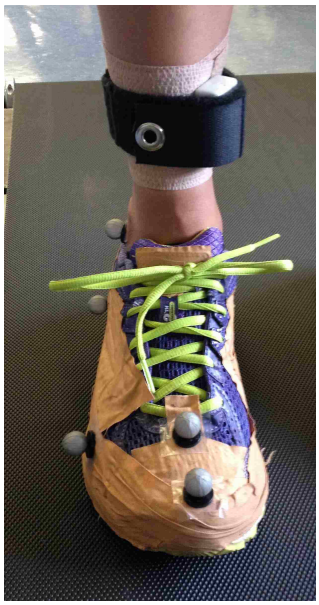

Figure 3.2: Accelerometer placement on the right tibia.

Retro-reflective markers were placed on each subject using double sided tape for the collection of motion capture data. Markers were positioned according to the lower body plug-in-gait model (VICON, Oxford, UK), seen in Figure 3.6. All marker placement was symmetrical on the left and right sides of the lower body. Pelvic markers were placed on

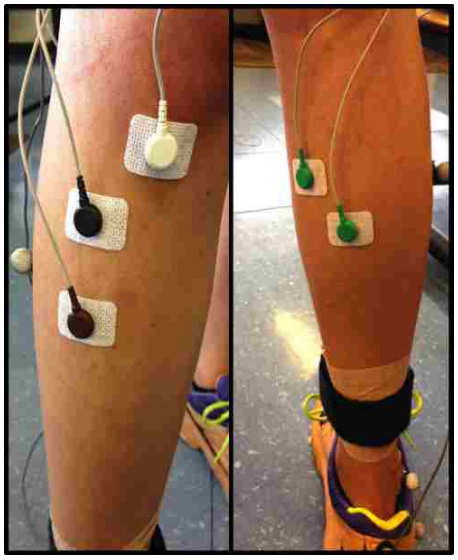

Figure 3.4: Electrodes on tibialis anterior and ground (left), and on medial gastrocnemius (right).

Figure 3.5: Sensor used to collect acceleration of right foot.

the anterior superior iliac spine and the posterior superior iliac spine. Leg markers were placed on the lateral surface of the thigh (at approximately the midpoint between the hip and the knee), on the lateral epicondyle of the knee, on the lateral surface of the upper 1/3 of the shank and on the lateral malleolus. Foot markers were adhered directly to the running shoe at the positions corresponding to the second metatarsal head and calcaneous (heel), with additional markers placed on the fifth metatarsal, medial distal phalanges (toe tip) and inferior lateral calcaneous (under ankle) of the right foot (Figure 3.14). In order to track the motion of the trunk (a surrogate for the center of mass), a marker was also placed on the sternum.

Figure 3.6: Retro-reflective marker (silver balls) placement on subject, surface electrodes (white rectangles) and acceleration monitoring unit (secured on medial right tibia with black strap) placement also shown.

3.3.2 Data collection

After the subject was outfitted with all of the data collection hardware, a static trial of retro-reflective marker position data was collected for each subject while they stood on the treadmill. This static data was used later in kinematic data analysis. Then each subject was instructed in how to safely get on and off the treadmill. Each individual then ran on the treadmill for two minutes to warm up and get used to running with the hardware attached to them. All treadmill running was done at 3.13 m/s. Following the warm up period, any necessary adjustments to the EMG leads were made to ensure subjects felt as natural as possible while running.

Before each trial, the acceleration monitoring unit was connected via Bluetooth to a laboratory laptop for data collection with a custom MATLAB program. Following Bluetooth connection, tibial acceleration data collection was initiated. Next, motion capture and EMG collection were both initiated. Once all data collection systems were running, the trial was ready to begin.

The subject began each trial standing with their feet on the floor on either side of the treadmill while the force plate was zeroed to ensure minimal drift during the data collection.

The individual then stomped three times on the center of the treadmill with their right foot. The three stomps were used to sync the tibial acceleration and ground reaction force data. The subject then returned their right foot to the original position. The treadmill was turned on to 3.13 m/s, the subject then got on as instructed and began running. In each trial the subject ran for five minutes. During the last 30 seconds of running, high speed video of the subject in the sagittal plane was collected (Figure 3.7).

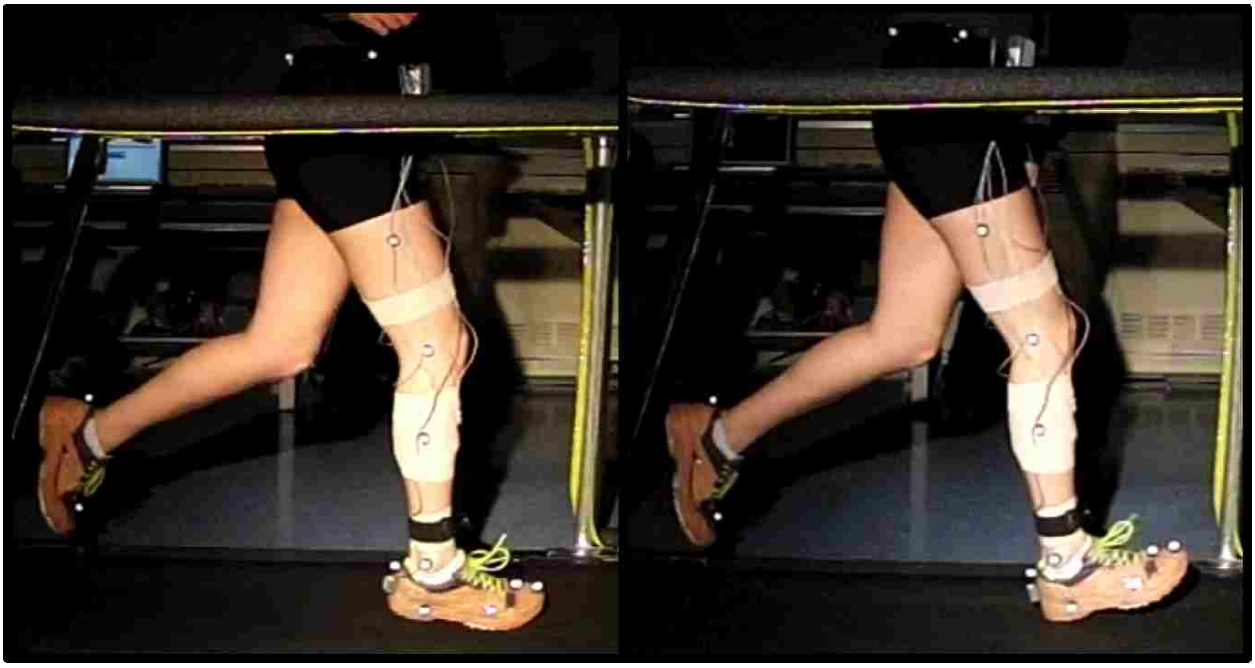

Figure 3.7: Subject running with nonrearfoot strike pattern (left) and rearfoot strike pattern (right).

For the first trial each subject was instructed to run naturally, during which time the subject's natural foot strike pattern was identified as either rearfoot or nonrearfoot striking. The subject's natural foot strike pattern was classified as either rearfoot or nonrearfoot according to foot strike angle (FSA) as defined by Altman and Davis [2], seen in Figure 2.1, where a FSA $> 8.0°$ indicated a rearfoot habitual pattern and FSA $< 8.0°$ indicated a nonrearfoot habitual pattern. Prior to the second trial each individual was instructed to attempt to change their foot strike pattern from rearfoot striking or nonrearfoot striking to the other pattern. If the subject was a natural rearfoot striker, they were instructed to "run more on your forefoot/toes." Natural nonrearfoot strikers were instructed to "run more on your rearfoot/heels." For the converted running trials, subjects were told to begin running with their natural foot strike and to transition when they felt comfortable. The subject then performed a practice trial in which they were able to try to convert their foot strike and get used to a different style of running. After practicing their altered foot strike pattern, a second trial was recorded in which the subject ran with the converted pattern.

3.4 Data analysis

3.4.1 Analysis theory

The subject's weight was entered in pounds and converted into kilograms to be used later in data analysis and normalization of variables to body weight. The five data files (kinematic and kinetic data from the static and running trials, and acceleration data from the running trial) were processed. The kinetic data from both trials contained force data (in volts) for four channels of the force plate mounted under the treadmill belt. The data from the four channels were added together to get a resultant vertical force for the static and running trials and converted from volts to Newtons. A peak finding routine was used to identify an initial stomp on the treadmill prior to the running trial in the force data. After the peak was found, the force array was shifted to begin at the index of the peak. The same routine was used to identify the stomp peak in the acceleration data, and then to shift that data array to begin at the peak index point. Then the kinematic data were trimmed from the beginning in order to synchronize with the kinetic and acceleration data.

Next a 4th order low-pass Butterworth filter was applied to the retro-reflective marker data in order to decrease noise. A fast Fourier transform (FFT) was used to find the appropriate cutoff frequency for filtering the marker data. A single-sided amplitude spectrum plot of the FTT showed a peak at 4.2 Hz, thus 10 Hz was chosen as the cutoff frequency for filtering. The MATLAB command filtfilt was used in order to achieve zero-phase filtering, which filtered the data in both the forward and reverse directions. After filtering, the marker data were then interpolated to increase the sampling rate from 100 Hz to 1000 Hz to match the sampling frequency of the force data. From the interpolated marker data, kinematics were then calculated by comparing marker positions from the static trial (neutral) to the running trial. Angles of interest were defined (Figure 3.8) and calculated as follows (anatomical locations refer to retro-reflective marker locations on subject, see Figure 3.6):

In the sagittal plane:

$$angle = \arctan(\frac{marker1_z - marker2_z}{marker1_y - marker2_y}) \tag{3.1}$$

where z = vertical position and y = horizontal position (along treadmill axis, see Figure 3.1).

1. Shank angle = ankle - knee (0 deg in standing)
2. Ankle angle = 5th metatarsal - ankle (90 deg in standing)
3. Foot strike angle = dorsum - heel (0 deg in standing)
4. Thigh angle = knee - hip (0 deg in standing)
5. Knee joint angle = thigh angle - shank angle (0 deg in standing)

In the frontal plane:

$$angle = \arctan(\frac{marker1_z - marker2_z}{marker1_x - marker2_x}) \tag{3.2}$$

where z = vertical position and x = horizontal position (across treadmill, side to side), angles in static position (standing) are defined as 0 deg.

1. Shank angle = ankle - knee
2. Thigh angle = knee - hip

Mid-line crossover was also calculated under both running conditions. This was defined as the retro-reflective marker on the dorsum of the right foot crossing over the mid-line between the two hip markers during running. The peak values of mid-line crossover were averaged to determine the average maximum crossover during running for each subject.

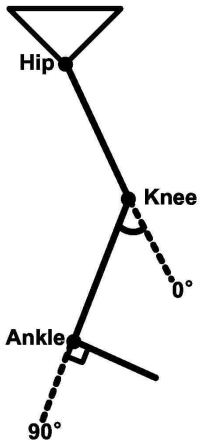

Figure 3.8: Joint angles as measured in the sagittal plane for the knee and ankle.

After the angles of interest were calculated, the force data were filtered using a fourth order low-pass Butterworth filter with a cut-off frequency of 50 Hz. The command filtfilt was again used to achieve zero-phase filtering. dF_z/dt was calculated from the filtered vertical force (F_z) data. The force data were processed sequentially, and using criteria (see below) four points were selected on each stance phase peak: the foot strike, first force peak, trough following first peak, major force peak and finally the toe off (Figure 3.9). While scanning the force data, certain selection criteria were defined for picking events. If the first criteria was met, the next criteria was checked, and if all criteria were met for a certain event, the point was selected. The selection criteria for each point of interest during stance were (where CI = current index in scanning of GRF data):

- Foot strike:
  1. $dF_z/dt(CI) > 8$ N/s
  2. $dF_z/dt(CI-1) < 8$ N/s
  3. $F_z(CI) < 100$ N
  4. The point at CI is picked as a foot strike (FS)
- First peak[1]:
  1. $dF_z/dt(CI) < 0$ N/s
  2. $CI - FS < 60$ mS, the distance between CI and the previously found FS is less than 60 mS
  3. The point at CI-1 is picked as a first peak (FP)
- Trough following first peak[1]:

1. $dF_z/dt(CI) > 0$ N/s
2. The point at CI-1 is picked as a trough

- Major peak:
  1. $dF_z/dt(CI) < 0$ N/s
  2. The point at CI-1 is picked as a major peak
- Toe off:
  1. $dF_z/dt(CI) > -1$ N/s
  2. $dF_z/dt(CI-1) < -1$ N/s
  3. $F_z(CI) < 100$ N
  4. The point at CI is picked as a toe off

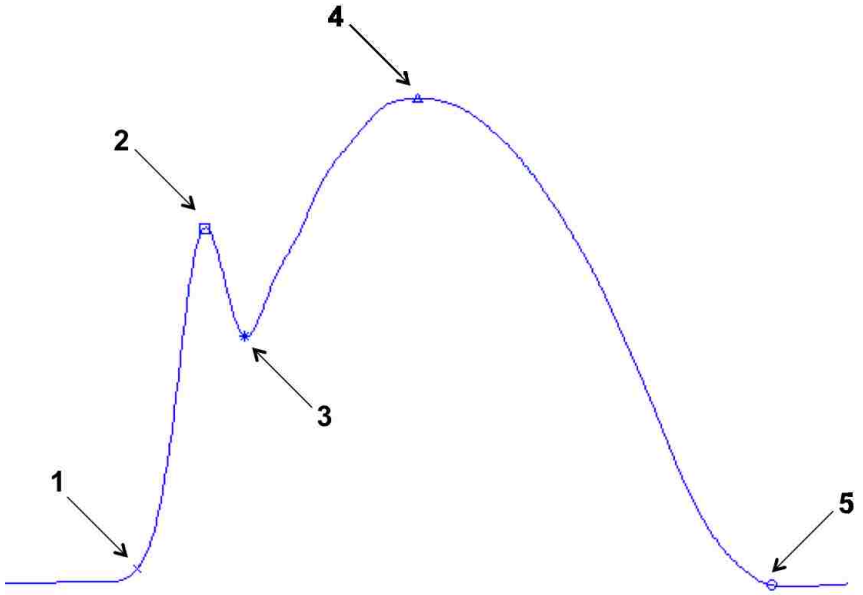

Figure 3.9: Events detected in GRF: (1) Foot strike (x), (2) First peak ($\square$), (3) Trough ($*$), (4) Major peak ($\triangle$), (5) Toe off (o).

After the foot strike events were found, the retro-reflective marker positions at these positions were identified from the kinematic data in order to track their location during foot strike. The average time that the first force peak occurred after the start of foot strike was calculated during the rearfoot strike pattern trial and then used to estimate the location in the nonrearfoot strike force data. The center of pressure (CoP) was estimated at the time of the first peak for each foot strike in order to calculate a "modified" ankle moment (Equation

[1]If a nonrearfoot strike pattern trial was being analyzed, there were no first peaks or troughs in the GRF data, and the identification and analysis for these variables was skipped.

3.3). Next the GRF was averaged across all foot strikes and normalized to 100 from the time of foot strike to toe off. From the time of each foot strike, and the previously calculated leg and foot angles of interest, angles were calculated from foot strike to toe off, and then averaged across all foot strikes. Average marker cycles were also determined by finding the marker location during each stance phase. From the average marker cycles, velocities of the center of mass, thigh, shank and ankle were calculated during foot strikes, and then averaged. All averaged kinematic variables were then normalized to 100.

3.4.2 Kinematic and kinetic analysis software

Program function

A custom analysis program and graphical user interface (GUI) was developed in MATLAB for processing of kinematic and kinetic data. Stance phase was defined as vertical GRF greater than 8 N. The program read in motion analysis data from the Nexus system and ground reaction force data from the force plate mounted under the treadmill belt. After the data were read in, retro-reflective marker data from the Nexus system were filtered using a fourth order low-pass Butterworth filter with a cut off frequency of 10 Hz, and then interpolated to increase the sampling frequency to that of the GRF data (1000 Hz). The GRF data were filtered using a fourth order low-pass Butterworth filter with a cut off frequency of 50 Hz to decrease background noise from the force plate. The program allowed the user to visualize and review the kinematic and kinetic data, as well as perform analysis of variables of interest.

Running the program

Once the program was initiated, the user was prompted to select five input files as follows:

1. Kinematic data from running trial
2. Kinetic data from running trial
3. Kinematic data from static calibration trial
4. Kinetic data from static calibration trial
5. Tibial acceleration data from running trial

From the initial static calibration two data files were selected for analysis: the retro-reflective marker data and GRF data. From the motion trial three data files were selected: marker data, GRF data and tibial acceleration data. After the static marker data was loaded, an initial plot of the ankle and heel marker data along with their average positions was made to ensure validity of the static trial. When the acceleration data were loaded, the user was prompted to plot the GRF and tibial acceleration data. When each data set was plotted, the user selected a point directly before an initial GRF peak, which was the result of the first of the subject's three initial stomps on the treadmill prior to the running trial. Using a peak detection routine, the time of the initial peak was determined in the tibial acceleration and GRF data (Figure 3.10).

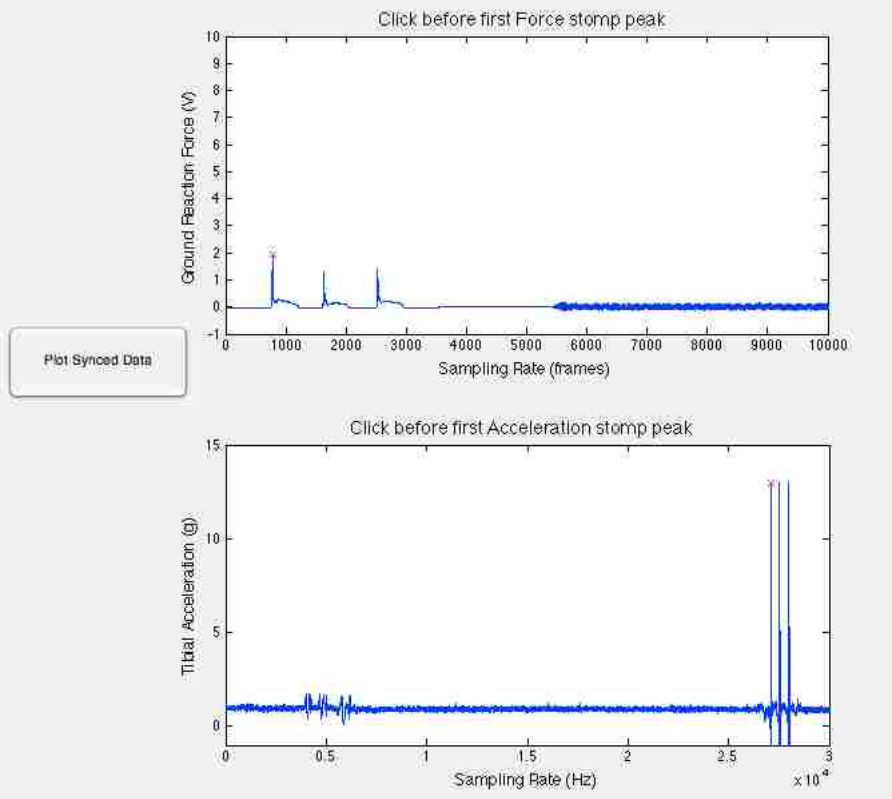

Figure 3.10: Screen shot from kinematic/kinetic analysis program, showing initial peaks chosen by peak finder routine (shown as red 'x'). Time points of the chosen peaks were used for synchronization of the marker and GRF data.

Next, a button on the GUI gave the user the option to plot the synced data. When this option was selected, retro-reflective marker data was first interpolated in order to increase the sampling rate to that of the GRF data. Then, the initial time point that was found from the peak detection routine was used to synchronize the GRF and tibial acceleration data sets. A plot of the two synchronized data sets was created for review (Figure 3.11). From the first frame of the static marker data file, a stick figure plot of the marker placement on the subject was created for visual confirmation.

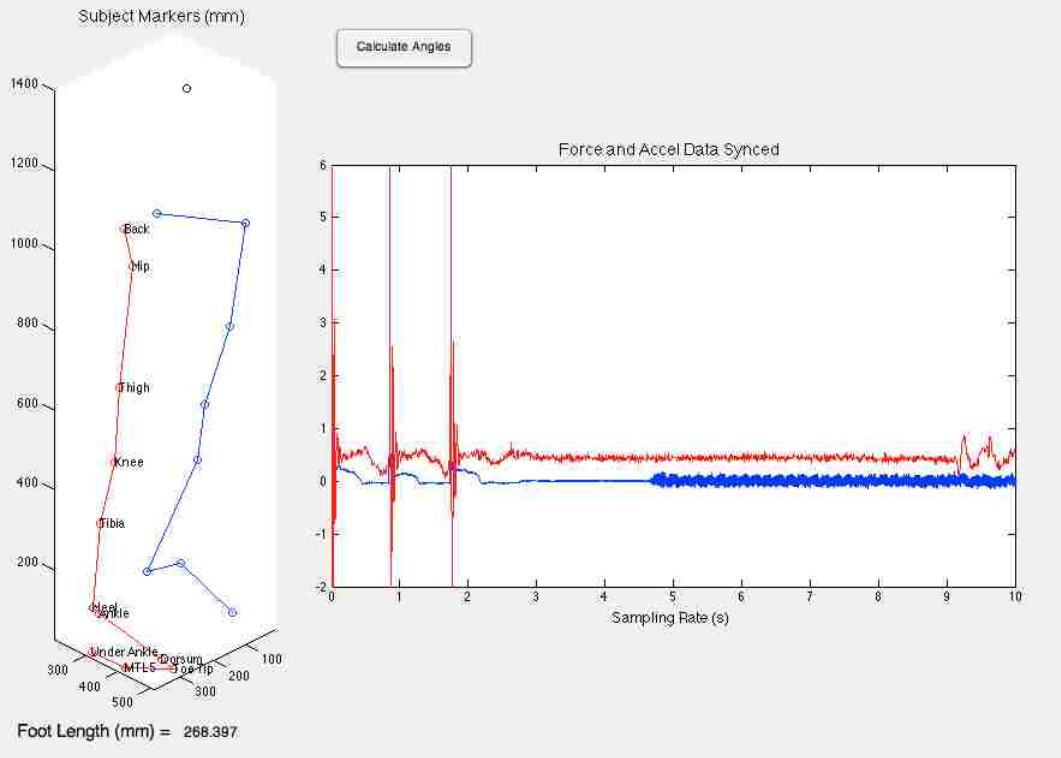

Figure 3.11: Screen shot from kinematic/kinetic analysis program, left: stick figure of marker positions on subject (right leg in red, left leg in blue), right: synced GRF (blue) and tibial acceleration (red) data.

Following the data synchronization, the user selected options to calculate angles from marker data and to filter the GRF data. Once the user selected the option to calculate angles, the newly interpolated marker data were used to calculate leg and foot angles of interest. When the filter force option was selected, the sum of the four F_z (vertical) output channels from the force plate was converted from units of volts to Newtons and filtered using a fourth order low-pass Butterworth filter with a 50 Hz cut off frequency. Following force filtering, a plot was created of the filtered force, the derivative of the force with respect to time (dF_z/dt) and the right heel marker data. The user was prompted to click at the start of a right foot strike that occurred after the GRF peak magnitude became constant, a result of the subject's natural running after lowering herself onto the treadmill. Right foot strikes were identified by the minimum points in the right heel marker data curve (Figure 3.12).

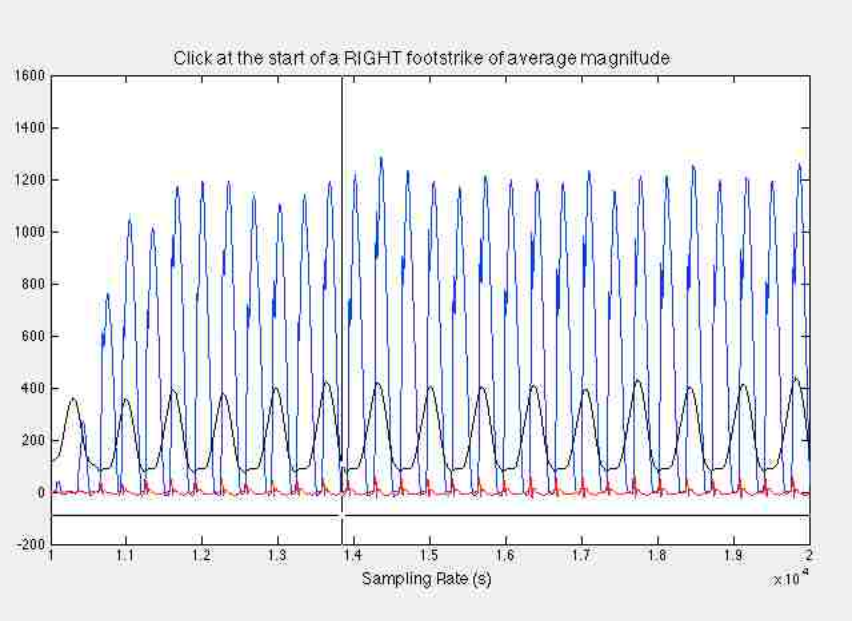

Figure 3.12: Screen shot from kinematic/kinetic analysis program, crosshair used to pick first stable right foot strike to use for analysis. GRF data in blue, GRF derivative in red and right ankle marker position in black.

After a right foot strike was selected, the program scanned through the GRF data to find events of interest during each stance phase using the criteria described in Section 3.4.1. The events that were selected included foot strike, first force peak, trough, major force peak and toe off (Figure 3.13). This data was used in the next section of the program: foot strike normalization.

The user was next prompted with an option to normalize foot strikes. This action produced two composite plots, one of all GRF foot strike curves (from foot strike to toe off) overlaid on each other, along with the average curve. The second plot was an overlay of all foot strike GRF curves normalized to 100, along with the average normalized GRF curve.

There were then six options for plot selection: angles vs. time, average angle cycles, average frontal angle cycles and sternal oscillation, marker cycles, segment velocities and normalized marker cycles. Each of these plot options allowed the user to review various parts of the data. After each plot option was reviewed, the average center of mass oscillation, average foot strike angle, average ankle joint moment and, for rearfoot running, average time of first force peak were shown on the GUI. Before exiting the program the user saved the data, which created two data files corresponding to the trial that was analyzed. One file was the Runner's Profile and one was the Model Input file, both of which are discussed in greater detail in section 3.4.3.

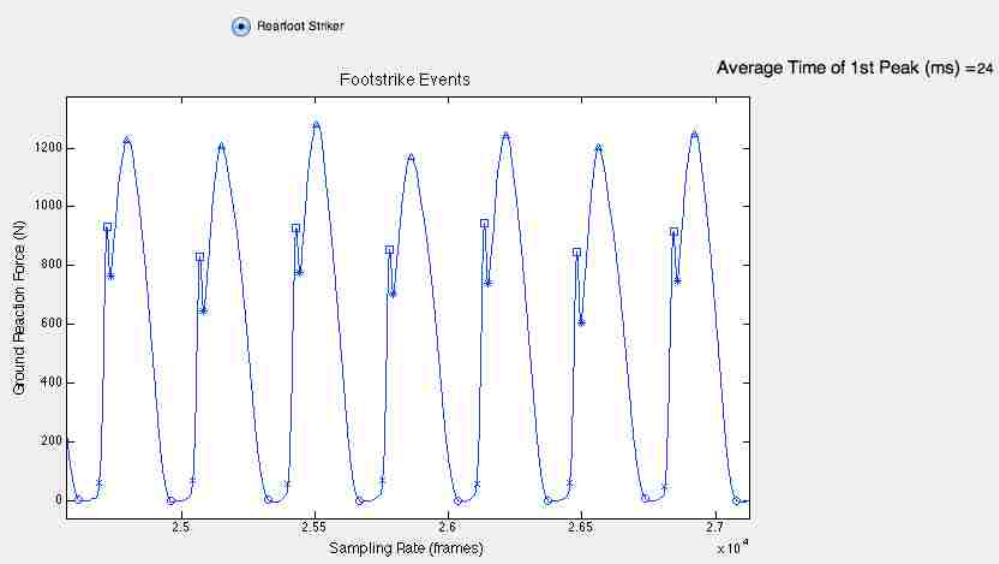

Figure 3.13: Screen shot from kinematic/kinetic analysis program, key foot strike points identified on GRF curve for rearfoot strike pattern ($x = startfootstrike$, $\square = firstpeak$, $* = trough$, $\triangle = majorpeak$, $o = endfootstrike$) and average time of first impact peak in stance phase.

3.4.3 Kinematics and kinetics

Motion analysis and ground reaction force data were run through the program described in section 3.4.2 for review, filtering and analysis. Variables of interests were vertical oscillation, foot strike angle (Figure 3.14), leg angle, shank angle, thigh angle, knee joint angle and ankle angle. These variables were all calculated during cycles of interest, which were defined from right foot strike to the next right foot strike for the length of the trial. The variable data cycles were then normalized to 100, and an average cycle was calculated for all the variables for each subject under both RFS and nRFS conditions. Similarly, for each trial, ground reaction force during stance phase (foot strike to toe off) was found for all foot strikes, each stance phase cycle was normalized to 100, and an average GRF cycle was calculated for each subject under both foot strike conditions.

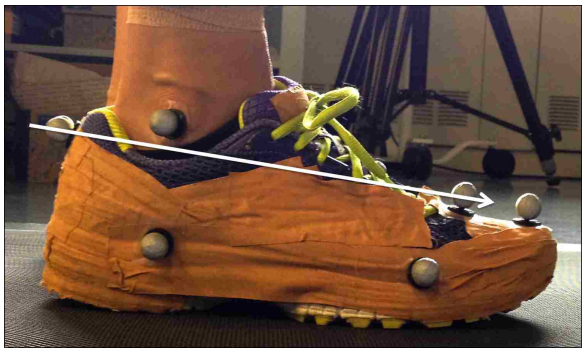

Figure 3.14: Retro-reflective marker placement on right foot and vector for foot strike angle calculation.

From each program run, two output files were created for each subject: a Runner's Profile file and a Model Input file. The Runner's Profile included the previously mentioned variables of interest averaged across all right foot strikes. The Model Input file contained average position and velocity data at foot strike for the center of mass (sternum), thigh, shank and ankle. These data will be used in future research for the development of a computational model for predicting individual impact, including tibial acceleration and GRF, during running. A Runner's Profile and Model Input file were produced for each subject's natural foot strike pattern and for their converted strike pattern, resulting in two Runner's Profiles and two Model Input files for each subject.

3.4.4 "Modified" ankle moment

The force plate used for GRF data collection only collected in the vertical (F_z) direction, and did not provide any data on shear forces during running. Because of this limitation, a "modified" ankle moment was calculated at the time of the initial GRF impact peak for each foot strike. In order to calculate the modified moment at the ankle, two assumptions were made:

1. The center of pressure of the foot is known or can be estimated.

2. All shear forces are negligible.

From these two assumptions, the center of pressure of the foot at the time of initial impact GRF peak was estimated. Foot length was calculated from the static trial motion analysis data as the distance from the heel to the toe marker (most anterior foot marker, Figure 3.14) for each subject. Using the calculated foot length, the center of pressure of the foot at the initial impact peak was designated to be 1/3 of the shoe length from the heel marker during running with a rearfoot strike pattern, and 2/3 of the shoe length from the heel marker when running with a nonrearfoot strike pattern.

First the time points of the initial GRF peaks were identified in the rearfoot strike pattern trial for each subject, both habitual rearfoot strikers and habitual nonrearfoot strikers running with a converted strike pattern. At each of the initial peak time points in the rearfoot strike pattern trial, the location of the center of pressure of the foot was then identified

from kinematic data. With the calculated center of pressure the ankle moment was then determined using an equation for ankle moment [29]:

$$\begin{aligned} M_{ankle}(i) &= F_y(i) \times ANKLE_z(i) + F_z(i) \times (CoP_y(i) - ANKLE_y(i)) \\ &\text{using assumptions 1 and 2, the equation becomes:} \\ &= F_z(i) \times (CoP_y(i) - ANKLE_y(i)) \end{aligned} \tag{3.3}$$

where i indicates the sample number, F_y is the anterior component of the ground reaction force, F_z is the vertical component of the ground reaction force, $ANKLE_y$ is the y-component of the ankle marker (see Figure 3.1 for lab axes definitions), $ANKLE_z$ is the z-component of the ankle marker, and CoP_y is the center of pressure of the ground reaction force in the direction of forward progression (y-direction).

During running with a nonrearfoot strike pattern, the GRF does not contain an initial impact peak. In order to approximate the time of impact in the nonrearfoot striking trials, the GRF impact peak times were averaged across all cycles for each subject's rearfoot striking trial. The average time of initial impact peak from a subject's rearfoot striking trial was then used in their nonrearfoot striking trial to identify the points in the GRF during stance phase at which to find the center of pressure of the foot. Once the center of pressure was determined by the method previously described, the ankle moment during nonrearfoot running was calculated (Equation 3.3).

3.4.5 Electromyography

EMG data for the tibialis anterior and the medial gastrocnemius were read into a custom MATLAB program for analysis. The program analyzed the data and found the muscle activation intervals from -0.4 seconds prior to each foot strike (occurring at $time = 0$) to 0.4 seconds after each foot strike. From these intervals, an average muscle activation was calculated for both the tibialis anterior and the medial gastrocnemius for each subject running with each of the two strike patterns. The average EMG data for both muscles during running with both strike types were then normalized for comparison between subjects. The maximum EMG value was identified for the medial gastrocnemius and the tibialis anterior in the rearfoot running trial for each subject. Normalization of the average EMG for both muscles under both foot strike conditions was accomplished by dividing all values by the maximum value, and then multiplying by 100. The average activation interval was calculated for the medial gastrocnemius and tibialis anterior, for RFS and nRFS conditions, across all subjects.

3.4.6 Tibial acceleration

Tibial acceleration data were analyzed in the same manner and with the same program as the EMG data. The acceleration monitoring unit that was affixed to the subject's right tibia collected data in three directions, A_x, A_y and A_z. The resultant tibial acceleration (A_r) and acceleration in the sagittal plane (A_xA_y) were calculated from the three components (Figure 3.15):

- A_x: acceleration along the long axis of the tibia

- A_y: acceleration along the anterior-posterior axis of the tibia
- A_z: acceleration along the medial-lateral axis of the tibia
- A_r: resultant acceleration
- A_xA_y: acceleration in the sagittal plane

The three components of acceleration were filtered at 255 Hz. A_y and A_z were then rotated by the previously calculated angle, $-\theta$, the angle of the sensor from the sagittal plane. Each component of the acceleration was then stored in intervals from -0.4 seconds prior to each foot strike (occurring at $time = 0$) to 0.4 seconds after each foot strike, and an average interval was determined. The average maximum value of acceleration was noted for comparison due to the implications in impact injury development.

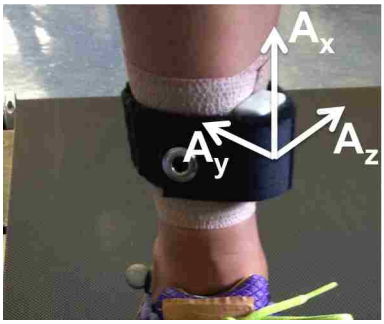

Figure 3.15: Axes of acceleration monitoring unit data collection

3.5 Statistical analysis

Kinematic variables of interest were normalized over a cycle from right foot strike through right swing phase (next right foot strike), ground reaction force was normalized over a cycle from foot strike to toe off, and electromyography and tibial acceleration data were normalized over an interval from -0.4 s prior to foot strike to 0.4 s after foot strike. The average of the normalized cycles/intervals was then determined for each subject for their RFS and nRFS running trials. In order to make comparisons between subjects and conditions, the average normalized cycle/interval was divided into 20 sections and the y value of the variable at each of the 20 x positions was determined for kinematic variables as well as EMG data. The observations at the 20 times of each dependent variable (e.g. foot angle) under the two conditions of the independent (within subjects) variable (strike pattern, i.e. RFS or nRFS) were used for paired samples t-tests. The variables that were found over the cycle of interest were:

- EMG
  - Tibialis anterior
  - Medial gastrocnemius

- Tibial acceleration
- Kinematics
  - Angles (sagittal plane): shank, thigh, knee, ankle, foot
  - Angles (frontal plane): shank, thigh
  - Velocities: center of mass, thigh, shank, ankle
- Ground reaction force

The following key research questions were identified and tested using a paired samples t-test for variables of interest in running with rearfoot and nonrearfoot strike pattern conditions:

- From hypothesis 1:
  1. Effect of foot strike type on activation time of medial gastrocnemius.
  2. Effect of foot strike type on activation magnitude of medial gastrocnemius.
- From hypothesis 2:
  1. Effect of foot strike type on number of peaks in medial gastrocnemius activity.
- From hypothesis 3:
  1. Effect of foot strike type on activation time of tibialis anterior.
  2. Effect of foot strike type on activation magnitude of tibialis anterior.
- From hypothesis 4:
  1. Effect of foot strike type on the magnitude of resultant tibial acceleration.

Chapter 4

Results

4.1 Subject exclusion

Three of the nine subjects tested (subjects 17, 25 and 47) were unsuccessful in changing their foot strike pattern during their respective testing session. Two of the three subjects had a habitual nRFS pattern and one subject had a habitual RFS pattern. This can be seen in Figure 4.1 where subjects 17, 25 and 47 did not show a significant change in foot angle from their habitual strike pattern (indicated by the circled 'x') to the non-habitual pattern (indicated by the un-circled 'x'). Because of this, these subjects were not included in the final data analysis for this study, and all further results will exclude their data as they would not be representative of a change in foot strike pattern.

As a result of the small sample size after subject exclusion ($n = 6$) and the multiple comparisons being made using paired samples t-tests (conducted for each kinematic variable and EMG at 20 points in the averaged cycle), there was an increased risk of finding false positives during statistical analysis. Because of this, the significance level was adjusted using a Bonferroni correction [7], where the p-value for significance was divided by the number of comparisons being made. After adjustment from the desired p-value (0.05), a critical p-value of 0.0025 was used for the comparisons of rearfoot and nonrearfoot variables at 20 points in the cycle. In subsequent figures of angles, velocities and EMG, comparisons that were significant at p-values of 0.005 and 0.01 are also displayed in order to show trends in data. Tibial acceleration and overall kinematic variables were also compared under both conditions using paired samples t-tests. However, since only one comparison was made for each component of acceleration and each overall kinematic variable (step length, center of mass oscillation, mid-line crossover), a critical p-value of 0.05 was used as an indication of significance in figures containing these data.

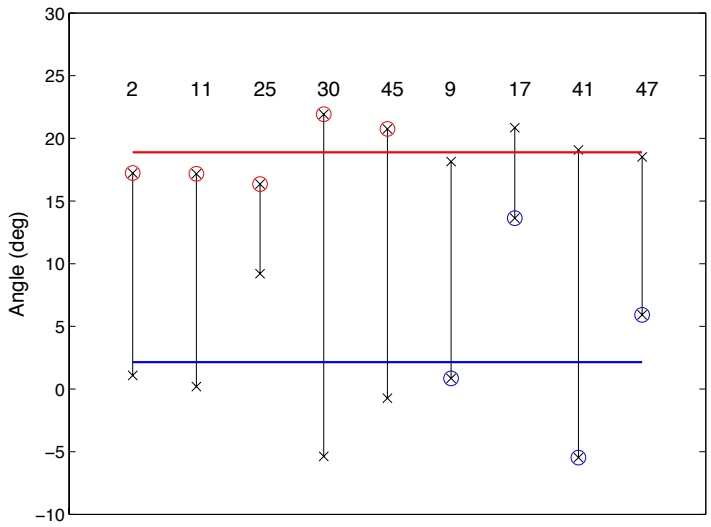

Figure 4.1: Foot angle at foot strike [2] for each subjects' attempt at RFS and nRFS running. Average foot angle shown for RFS and nRFS conditions as red and blue lines, respectively. Average foot angles indicated by 'x', and subjects' average foot angle while using habitual strike pattern indicated by the circled 'x'.

4.2 Kinematics

Kinematic variables were observed both as individual values at the time of foot strike, and over an averaged, normalized cycle of interest (average cycle), which began at right foot strike, included right foot stance and swing phase and ended at the time of the following right foot strike. Step length, center of mass oscillation and mid-line crossover were observed over the entirety of each trial and then averaged. All graphs of kinematic variables shown below contain data averaged across all subjects for RFS (in red) and nRFS (in blue) running. To maintain the location of toe off in the average cycle, the average time of toe off in the cycle was found as a percentage of cycle time, with 0% indicating foot strike and 100% indicating the end of the swing phase. The percent of cycle where toe off occurred was averaged across all subjects for the RFS and nRFS conditions and found to be 52% (indicated in figures by a vertical black line). In order to determine where the RFS and nRFS conditions were statistically different for the variables of interest, the average variable cycles for each subject under both strike conditions were divided into 20 sections. For each variable of interest, the value at each division was saved for comparison between subjects and foot strike conditions. These individual values are plotted along with the average cycle for each variable in the subsequent figures.

4.2.1 Overall

The average step length, center of mass (CoM) oscillation from highest to lowest point during running and mid-line crossover were averaged across each trial. Additionally, a modified ankle moment was calculated at the time of foot strike, and averaged to get an average foot strike modified ankle moment for each condition. Step length was not found to be significantly different (seen in Table 4.1), p-value= 0.07, which suggests that any changes in kinematics between RFS and nRFS running were not the result of a significant change in step length. CoM oscillation and mid-line crossover were similar between both conditions, p-value= 0.74 and 0.82, respectively. The average modified ankle moment at foot strike was significantly greater in nRFS compared to RFS, p-value= 0.001.

Table 4.1: Step length, CoM oscillation, mid-line crossover and ankle moment averaged for RFS and nRFS conditions across all subjects. Significant differences between conditions are indicated by $*$ (p= 0.05).

FS Type	Step Length (m)	CoM Oscillation (mm)	Mid-line Crossover (mm)	Ankle Moment (Nm/kg)($*$)
Rearfoot	1.128 ± 0.085	90.560 ± 20.837	106.128 ± 22.024	0.434 ± 0.111
Nonrearfoot	1.097 ± 0.076	88.970 ± 15.295	106.407 ± 23.185	2.039 ± 0.196

4.2.2 At foot strike

Kinematic variables of interest were calculated at the time of all right foot strikes under both foot strike conditions for each subject. The variables were then averaged across all subjects for both foot strike conditions, seen in Tables 4.2 and 4.3.

Table 4.2: Lower extremity angles at the time of foot strike in the sagittal plane during RFS and nRFS conditions. Significant differences between conditions are indicated by $*$ (p= 0.0025), $\times$ (p= 0.005) and $\circ$ (p= 0.01).

Sagittal Angles (deg)					
FS Type	Foot($*$)	Knee	Ankle($*$)	Shank	Thigh
Rearfoot	19.049 ± 1.939	14.731 ± 5.680	102.460 ± 1.887	6.590 ± 2.573	21.321 ± 3.386
Nonrearfoot	-1.575 ± 3.044	15.400 ± 7.253	82.625 ± 6.136	5.800 ± 3.648	21.200 ± 4.094

4.2.3 Stance and swing phase

Stance phase was defined as the time from right foot strike to right toe off, as seen in Figure 4.2 where foot strike occurs at $cycletime = 1$, and toe off occurs at $cycletime = 52$ (indicated by the vertical black line). Swing phase was defined as the time from right toe off to the next right foot strike (Figure 4.14), where normalized $cycletime = 100$ indicates the next right foot strike and thus the end of the swing phase.

Foot angle (0 deg standing, angle $>$ 0 deg= dorsiflextion, angle $<$ 0 deg= plantar flexion) at foot strike was significantly greater in the RFS condition (Figure 4.3) as the subjects were

Table 4.3: Lower extremity angles at the time of foot strike in the frontal plane during RFS and nRFS conditions. Significant differences between conditions are indicated by $*$ (p= 0.0025), $\times$ (p= 0.005) and $\circ$ (p= 0.01).

Frontal Angles (deg)		
FS Type	Shank	Thigh($\times$)
Rearfoot	-4.510 ± 1.044	-6.038 ± 1.147
Nonrearfoot	-4.536 ± 0.954	-4.819 ± 1.561

dorsiflexed in order to achieve a rearfoot strike, which was not the case in the nRFS trial (Figure 4.2). At foot strike under the nRFS condition subjects showed significantly greater plantar flexion, resulting in a smaller foot angle. The foot angle in the RFS condition then decreased until 20% of stance, when it became similar to that of the nRFS condition for the rest of stance phase. Foot angle was similar at the beginning of swing phase in RFS and nRFS. At 50% of swing phase, as the RFS condition prepared for dorsiflexion needed at foot strike, the foot angle became significantly larger in the RFS condition.

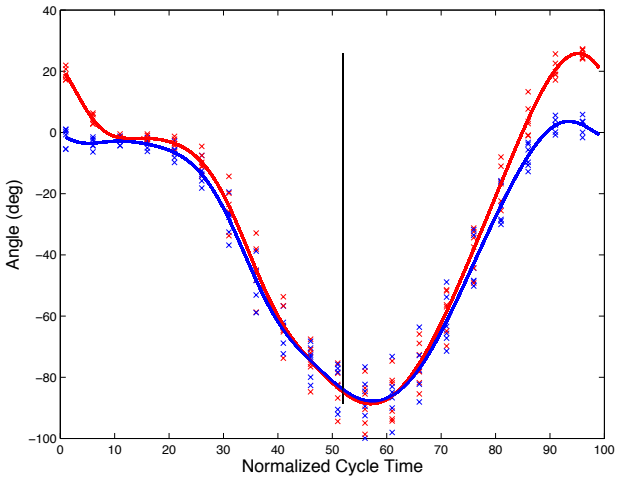

Figure 4.2: Foot angle for RFS (red) and nRFS (blue) conditions, toe off is indicated by vertical black line. Individual subject values are shown at each time point and indicated by a red and blue 'x' for RFS and nRFS conditions, respectively.

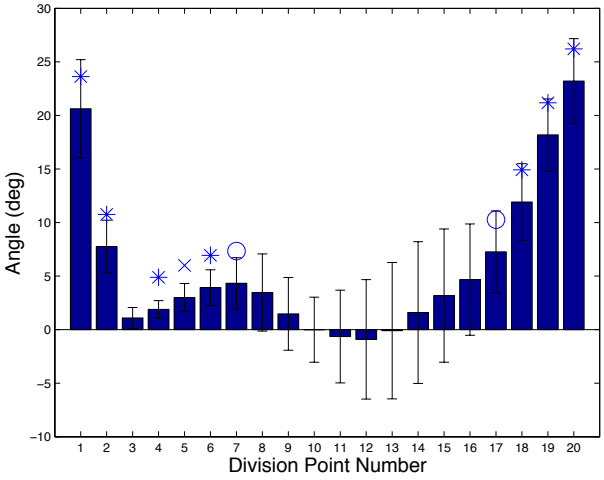

Figure 4.3: Differences (RFS-nRFS) in foot angle at 20 points on the average cycle. The average RFS value for all subjects at each point was subtracted from its corresponding value in the nRFS condition. Error bars represent the standard deviation of the differences. Significant differences between conditions are indicated by $*$ (p= 0.0025), $\times$ (p= 0.005) and $\circ$ (p= 0.01). Foot strike, toe off and the end of swing phase occurred at points 1, 11 and 20, respectively.

Ankle angle (90 deg standing, angle $>$ 90 deg = dorsiflexion, angle $<$ 90 deg = plantar flexion) was significantly greater in the RFS condition at foot strike (Figure 4.5) and remained considerably larger for the first 80% of stance phase (Figure 4.4). There was no significant difference in ankle angle during mid-stance (while the foot is relatively flat) through toe off. Ankle angle was similar in both conditions during the beginning of swing phase, but shows an significant increase in angle toward the end of swing phase in the RFS condition as the ankle dorsiflexes to prepare for foot strike, while the nRFS ankle angle decreases as plantar flexion occurrs.

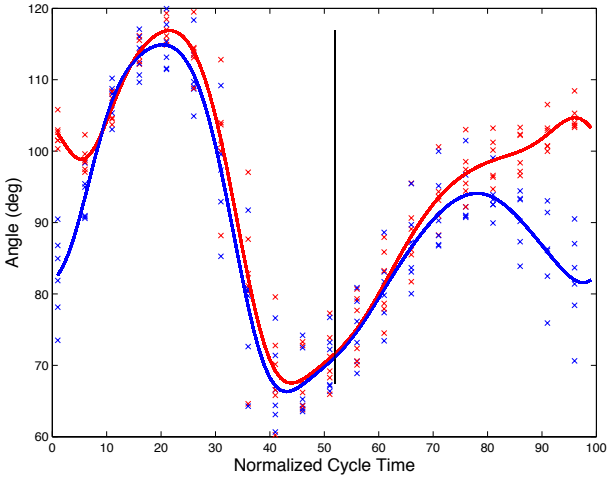

Figure 4.4: Ankle angle for RFS (red) and nRFS (blue) conditions, toe off is indicated by vertical black line. Individual subject values are shown at each time point and indicated by a red and blue 'x' for RFS and nRFS conditions, respectively.

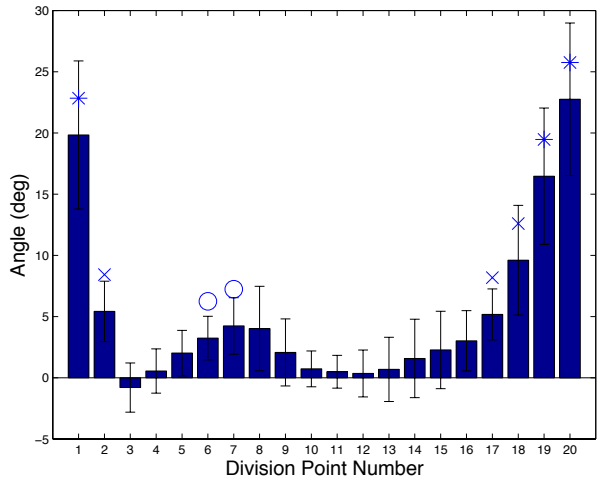

Figure 4.5: Differences (RFS-nRFS) in ankle angle at 20 points on the average cycle. The average RFS value for all subjects at each point was subtracted from its corresponding value in the nRFS condition. Error bars represent the standard deviation of the differences. Significant differences between conditions are indicated by $*$ (p= 0.0025), $\times$ (p= 0.005) and $\circ$ (p= 0.01). Foot strike, toe off and the end of swing phase occurred at points 1, 11 and 20, respectively.

Knee angle (0 deg standing, angle $>$ 0 deg = flexion), Figure 4.6, showed no significant differences (Figure 4.7) between conditions during stance or swing phase. The similarity in knee angle over the entirety of stance and swing phase indicates that the kinematic differences seen between foot strike patterns were all modulated at the foot and ankle.

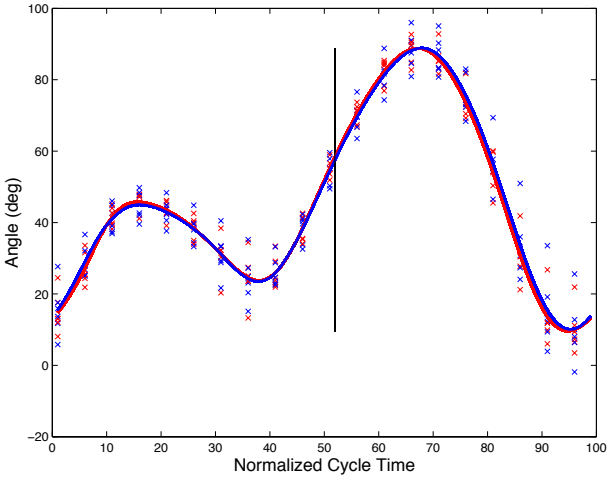

Figure 4.6: Knee angle for RFS (red) and nRFS (blue) conditions, toe off is indicated by vertical black line. Individual subject values are shown at each time point and indicated by a red and blue 'x' for RFS and nRFS conditions, respectively.

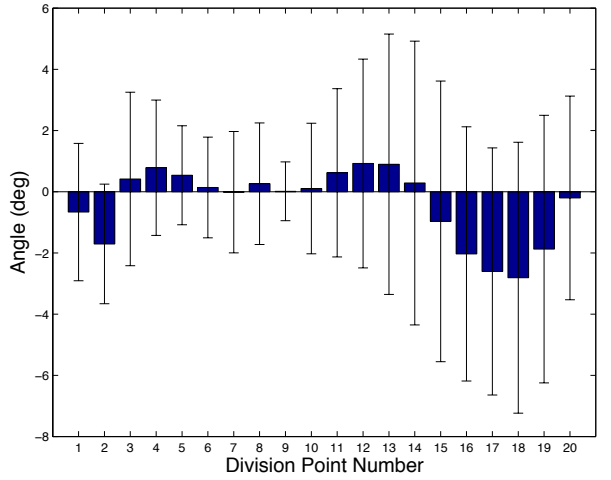

Figure 4.7: Differences (RFS-nRFS) in knee angle at 20 points on the average cycle. The average RFS value for all subjects at each point was subtracted from its corresponding value in the nRFS condition. Error bars represent the standard deviation of the differences. No significant differences were found for knee angle between conditions. Foot strike, toe off and the end of swing phase occurred at points 1, 11 and 20, respectively.

Shank angle was similar for both conditions (Figure 4.8) for the majority of stance and swing phase. However, at the second division point the angle was significantly greater (critical $p-value = 0.005$) in the RFS condition (Figure 4.9). Because this only occurred at one point division in the shank angle, it may or may not be seen with a larger sample size.

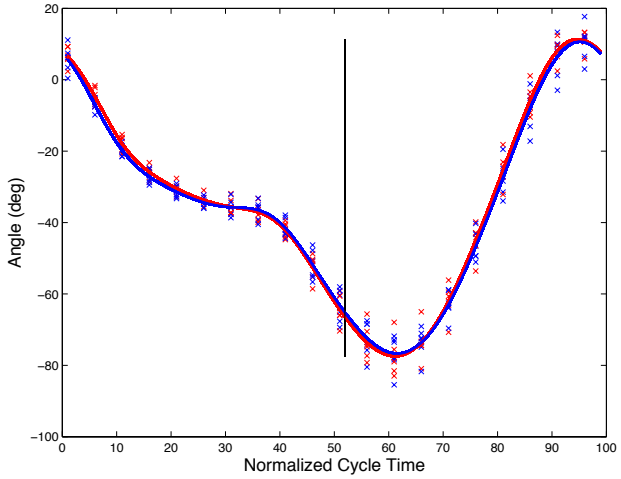

Figure 4.8: Shank angle for RFS (red) and nRFS (blue) conditions, toe off is indicated by vertical black line. Individual subject values are shown at each time point and indicated by a red and blue 'x' for RFS and nRFS conditions, respectively.

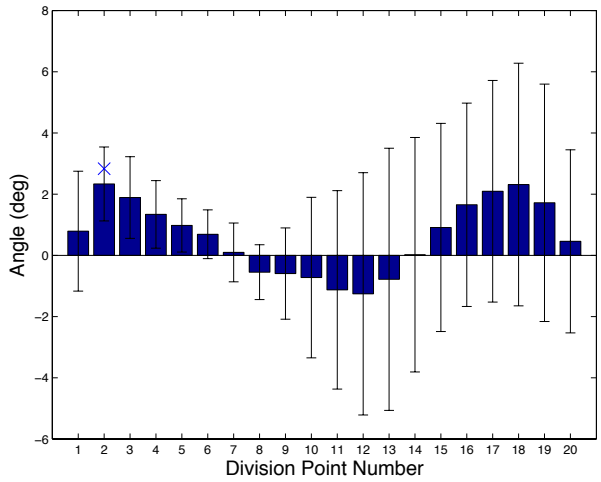

Figure 4.9: Differences (RFS-nRFS) in shank angle at 20 points on the average cycle. The average RFS value for all subjects at each point was subtracted from its corresponding value in the nRFS condition. Error bars represent the standard deviation of the differences. Significant differences between conditions are indicated by $*$ (p= 0.0025), $\times$ (p= 0.005) and $\circ$ (p= 0.01). Foot strike, toe off and the end of swing phase occurred at points 1, 11 and 20, respectively.

Shank frontal angle (Figure 4.10) was not significantly different between the RFS and nRFS conditions. High across subject variability was observed in the shank frontal angle following toe off (Figure 4.11), with some subjects having a positive angle, and others having a negative angle. This was potentially the result of certain subjects pronating, during which

time the ankle rolls toward the mid-line, thus causing a smaller (or negative) frontal angle of the shank. In contrast, some subjects may have been prone to supination during toe off, causing the ankle to roll away from the mid-line, and resulting in a larger frontal angle of the shank.

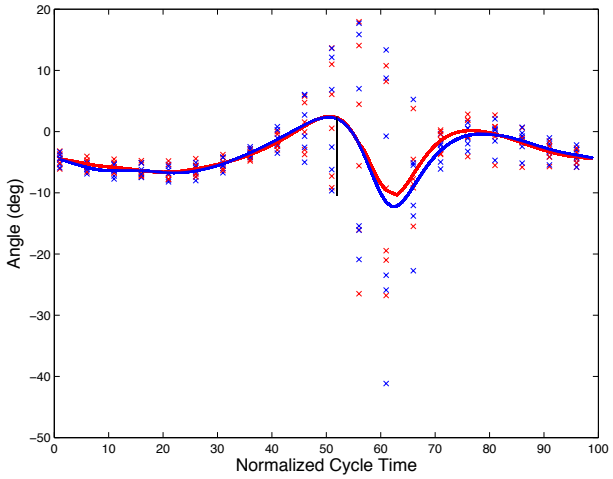

Figure 4.10: Shank frontal angle for RFS (red) and nRFS (blue) conditions, toe off is indicated by vertical black line. Individual subject values are shown at each time point and indicated by a red and blue 'x' for RFS and nRFS conditions, respectively.

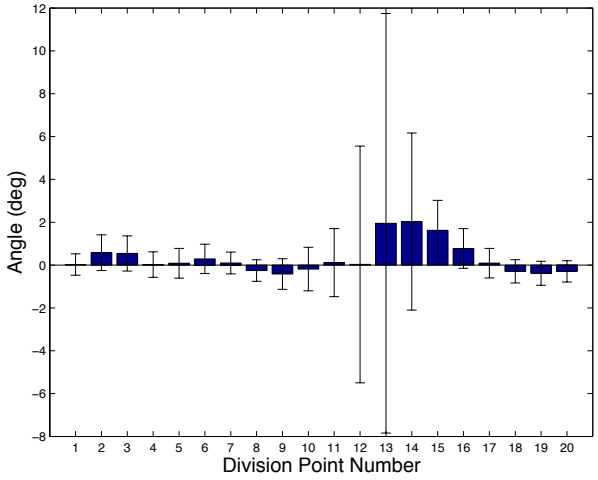

Figure 4.11: Differences (RFS-nRFS) in shank angle in the frontal plane at 20 points on the average cycle. The average RFS value for all subjects at each point was subtracted from its corresponding value in the nRFS condition. Error bars represent the standard deviation of the differences. No significant differences were found for shank frontal angle between conditions. Foot strike, toe off and the end of swing phase occurred at points 1, 11 and 20, respectively.

Thigh angle (Figure 4.12) was not significantly different between the RFS and nRFS conditions, as seen in Figure 4.13.

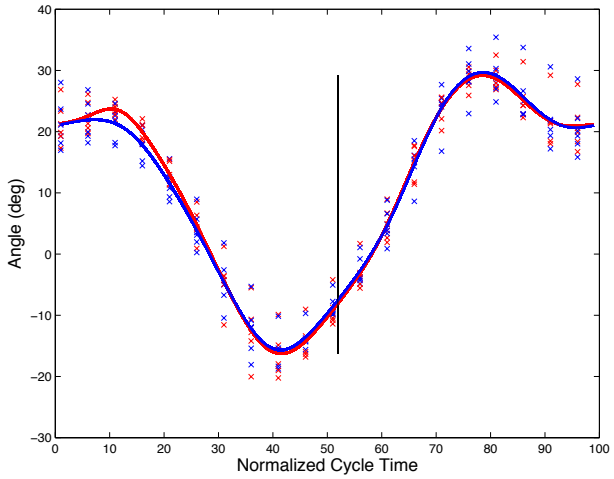

Figure 4.12: Thigh angle for RFS (red) and nRFS (blue) conditions, toe off is indicated by vertical black line. Individual subject values are shown at each time point and indicated by a red and blue 'x' for RFS and nRFS conditions, respectively.

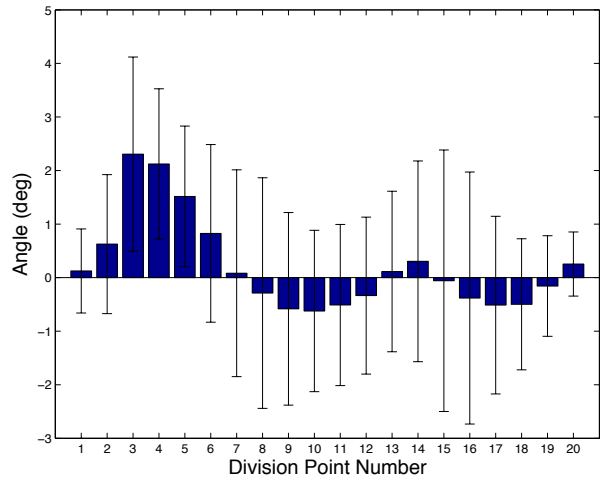

Figure 4.13: Differences (RFS-nRFS) in thigh angle at 20 points on the average cycle. The average RFS value for all subjects at each point was subtracted from its corresponding value in the nRFS condition. Error bars represent the standard deviation of the differences. No significant differences were found for thigh angle between conditions. Foot strike, toe off and the end of swing phase occurred at points 1, 11 and 20, respectively.

Thigh frontal angle (Figure 4.14) was significantly more negative (knee angled toward the mid-line) at and just before foot strike in the RFS condition. This is likely due to an

inversion of the foot and extension of the knee during foot strike in RFS running. In contrast, the thigh frontal angle was significantly greater in the nRFS condition at the time of foot strike and immediately before foot strike occurred (Figure 4.15). This was the result of an increase in hip and thigh flexion at foot strike during nRFS running.

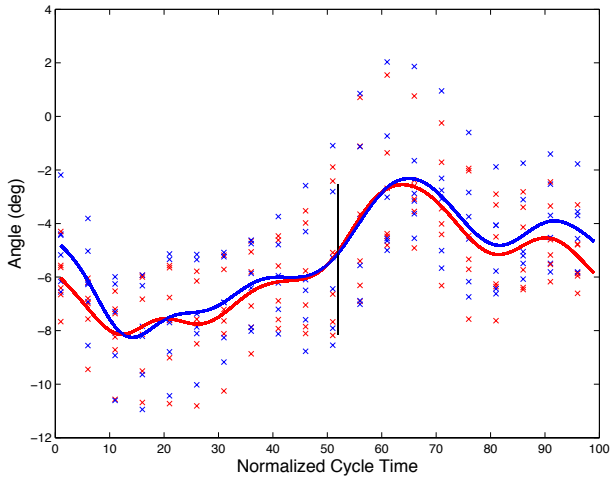

Figure 4.14: Thigh frontal angle for RFS (red) and nRFS (blue) conditions, toe off is indicated by vertical black line. Individual subject values are shown at each time point and indicated by a red and blue 'x' for RFS and nRFS conditions, respectively.

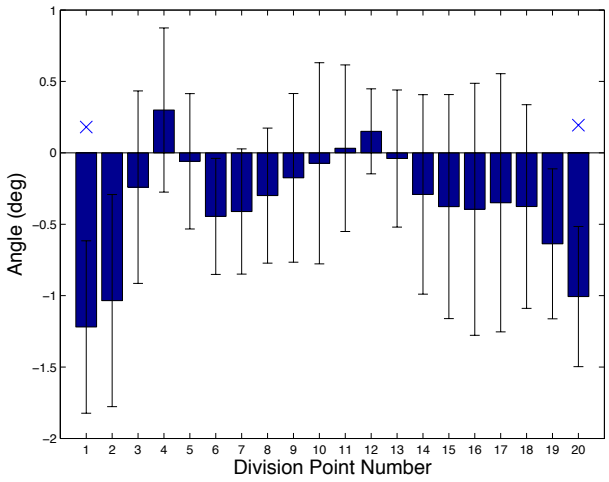

Figure 4.15: Differences (RFS-nRFS) in thigh angle in the frontal plane at 20 points on the average cycle. The average RFS value for all subjects at each point was subtracted from its corresponding value in the nRFS condition. Error bars represent the standard deviation of the differences. Significant differences between conditions are indicated by $*$ (p= 0.0025), $\times$ (p= 0.005) and $\circ$ (p= 0.01). Foot strike, toe off and the end of swing phase occurred at points 1, 11 and 20, respectively.

4.2.4 Angle-Angle diagrams

Thigh-knee (Figure 4.16) and knee-ankle (Figure 4.17) diagrams were created to show how the respective joint angles vary over time in relation to each other. Figure 4.16 shows thigh angle on the x-axis, plotted against knee angle on the y-axis for each subject under RFS (red) and nRFS (blue) conditions. Knee angle is defined as 0 deg in standing, and as the knee flexes, the angle increases in magnitude (shown as becoming more negative in Figure 4.16). Thigh angle is defined as 0 deg in standing, greater than 0 deg during flexion and less than 0 deg during extension. Figure 4.17 shows ankle angle on the x-axis, plotted against knee angle on the y-axis for each subject under RFS (red) and nRFS (blue) conditions. Ankle angle is defined as 90 deg in standing, greater than 90 deg during dorsiflexion and less than 90 deg during plantar flexion.

Angle-angle diagrams allow for the observation of changes in coordination. The change in knee angle with respect to thigh angle can be seen for each subject and both conditions in Figure 4.16. Sub-plots 3 and 6 show no difference in coordination between RFS (red) and nRFS (blue), as the two curves are highly similar. Sub-plots 1, 2 and 4 show decreased coordination in the nRFS condition, which is indicated by a decrease in the amount of change of the thigh angle while the knee angle is changing as the knee is flexes. Sub-plot 5 shows an overall decrease in coordination in the RFS condition, which is indicated by an overall smaller angle range. The change in knee angle with respect to ankle angle is shown in Figure 4.17. All sub-plots show distinct differences between RFS (red) and nRFS (blue) conditions, as seen by the small amount of overlap between the two curves. In the RFS condition, as the knee flexes the ankle dorsiflexes, which is indicated by a shift to the right in the RFS curves. In contrast, in the nRFS condition, as the knee flexes the ankle plantar flexes, which can be seen in the left shift of the nRFS curves.

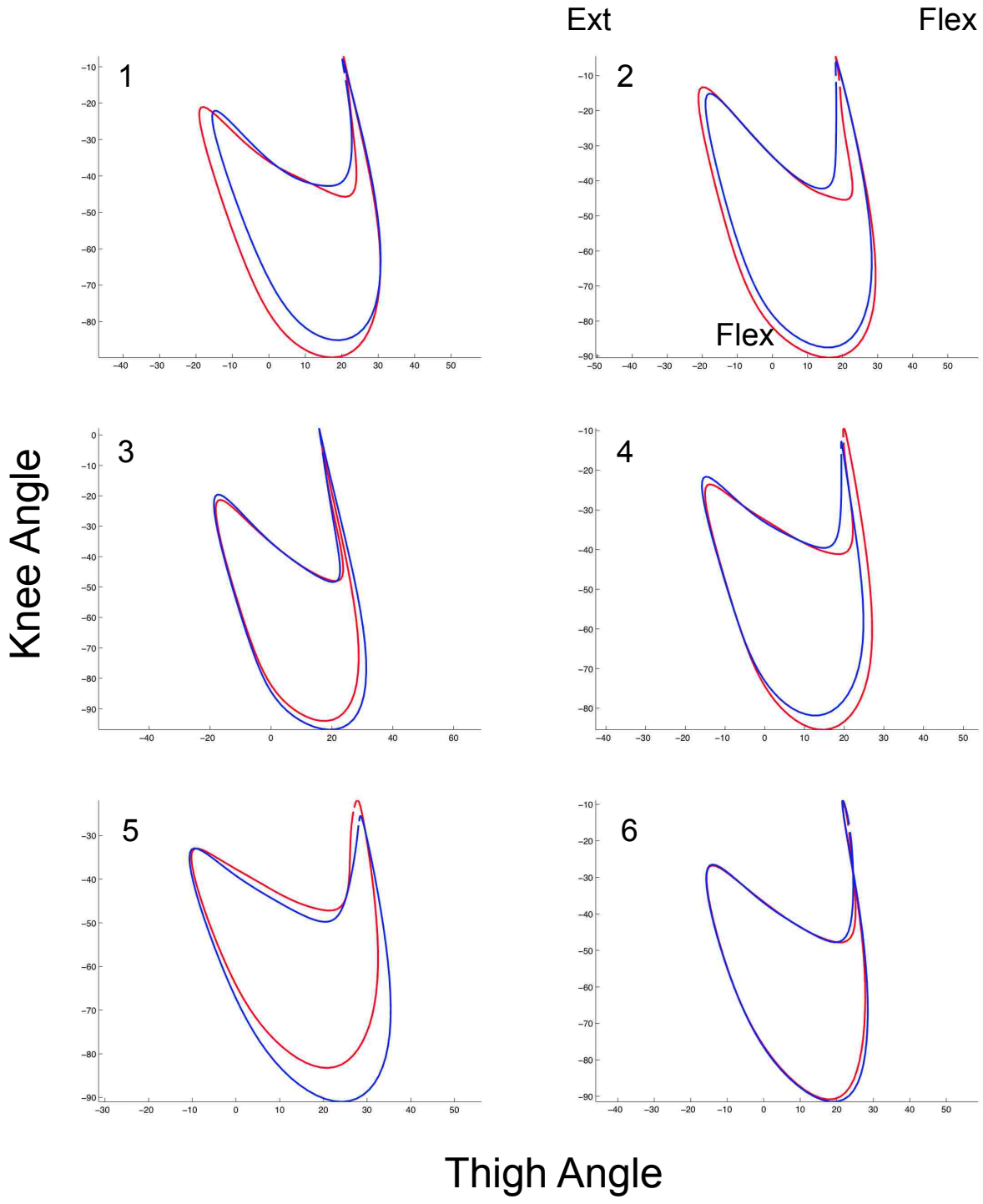

Figure 4.16: Thigh-knee angle diagrams for each subject under RFS (red) and nRFS (blue). Thigh angle shown on the x-axis and knee angle on the y-axis. The change in knee angle relative to the change in thigh angle was an indication of overall coordination. Subjects in sub-plots 2 and 5 were habitual nRFS.

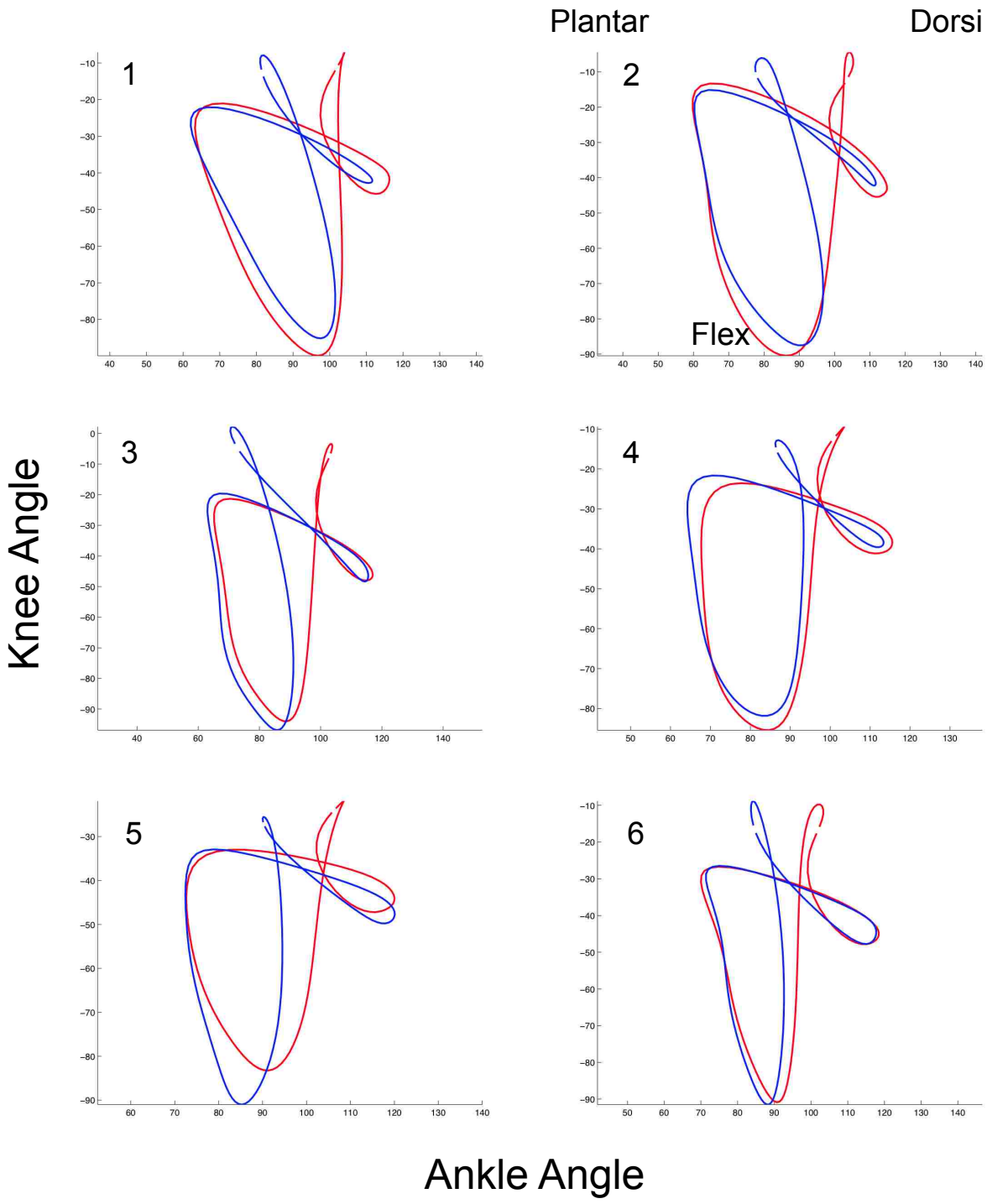

Figure 4.17: Ankle-knee angle diagrams for each subject under RFS (red) and nRFS (blue). Ankle angle shown on the x-axis and knee angle on the y-axis. The change in knee angle relative to the change in ankle angle was an indication of overall coordination of the movement of these two joints. Subjects in sub-plots 2 and 5 were habitual nRFS.

4.3 Velocity

Segment velocities were calculated during the same average cycle as the kinematic variables, from right foot strike to the following right foot strike. The velocity of the center of mass (sternum) was similar for both RFS and nRFS conditions during stance and swing phase (Figure 4.18).

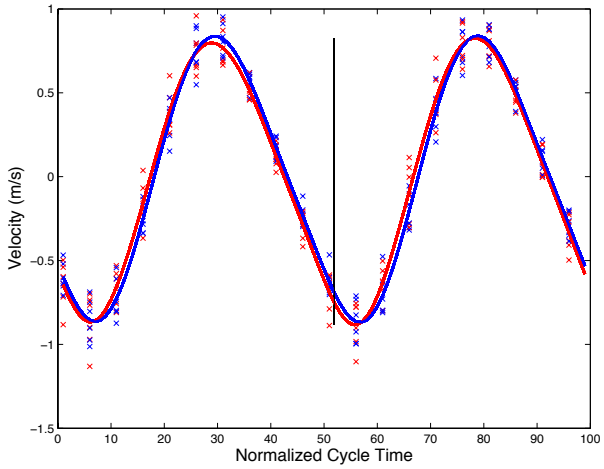

Figure 4.18: Velocity of the center of mass (sternum) for RFS (red) and nRFS (blue) conditions, toe off is indicated by vertical black line. Individual subject values are shown at each time point and indicated by a red and blue 'x' for RFS and nRFS conditions, respectively.

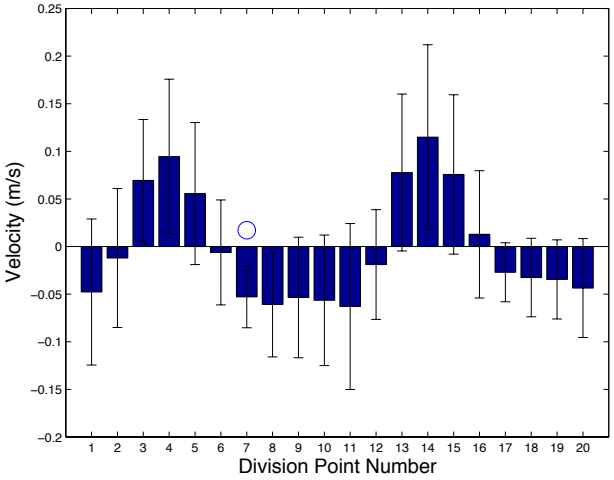

Figure 4.19: Differences (RFS-nRFS) in CoM velocity at 20 points on the average cycle. The average RFS value for all subjects at each point was subtracted from its corresponding value in the nRFS condition. Error bars represent the standard deviation of the differences. Significant differences between conditions are indicated by $\circ$ (p= 0.01). Foot strike, toe off and the end of swing phase occurred at points 1, 11 and 20, respectively.

Thigh velocity (Figure 4.20) was similar for both conditions at the time of foot strike, but became significantly greater in the RFS condition at the two time points following foot strike, seen in Figure 4.21.

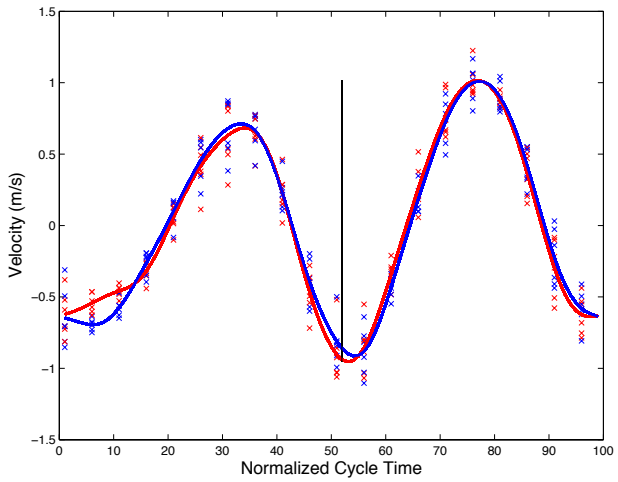

Figure 4.20: Velocity of the thigh for RFS (red) and nRFS (blue) conditions, toe off is indicated by vertical black line. Individual subject values are shown at each time point and indicated by a red and blue 'x' for RFS and nRFS conditions, respectively.

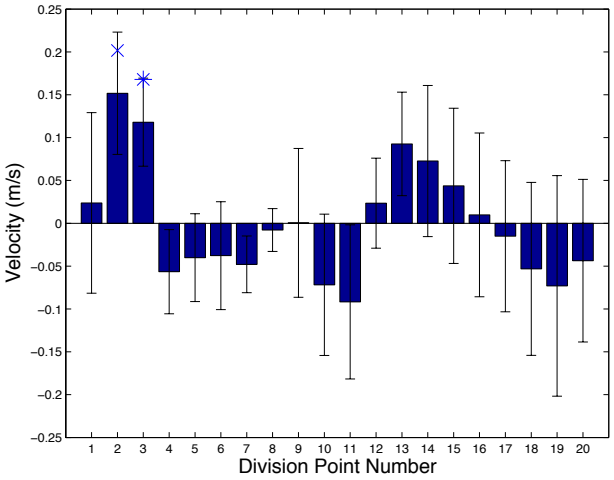

Figure 4.21: Differences (RFS-nRFS) in thigh velocity at 20 points on the average cycle. The average RFS value for all subjects at each point was subtracted from its corresponding value in the nRFS condition. Error bars represent the standard deviation of the differences. Significant differences between conditions are indicated by $*$ (p= 0.0025), $\times$ (p= 0.005) and $\circ$ (p= 0.01). Foot strike, toe off and the end of swing phase occurred at points 1, 11 and 20, respectively.

Shank velocity (Figure 4.22) was significantly greater in magnitude at the time point following foot strike and at the time of toe off for the RFS condition (Figure 4.23). For the rest of the cycle the shank velocity was similar for the two conditions.

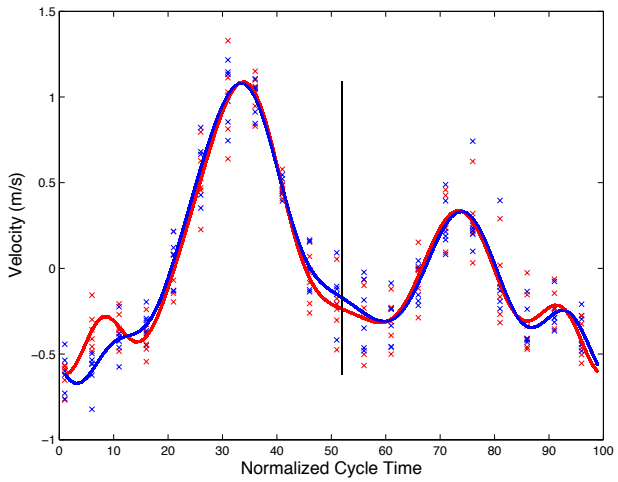

Figure 4.22: Velocity of the shank for RFS (red) and nRFS (blue) conditions, toe off is indicated by vertical black line. Individual subject values are shown at each time point and indicated by a red and blue 'x' for RFS and nRFS conditions, respectively.

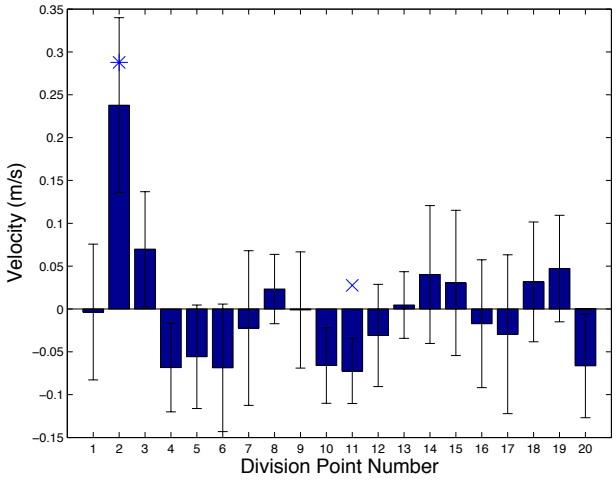

Figure 4.23: Differences (RFS-nRFS) in shank velocity at 20 points on the average cycle. The average RFS value for all subjects at each point was subtracted from its corresponding value in the nRFS condition. Error bars represent the standard deviation of the differences. Significant differences between conditions are indicated by $*$ (p= 0.0025), $\times$ (p= 0.005) and $\circ$ (p= 0.01). Foot strike, toe off and the end of swing phase occurred at points 1, 11 and 20, respectively.

Ankle velocity (Figure 4.24) showed a trend toward being significantly greater in magnitude for the RFS condition at the two time points following foot strike (Figure 4.25). During the rest of stance and swing phase the ankle velocity was similar for the two conditions.

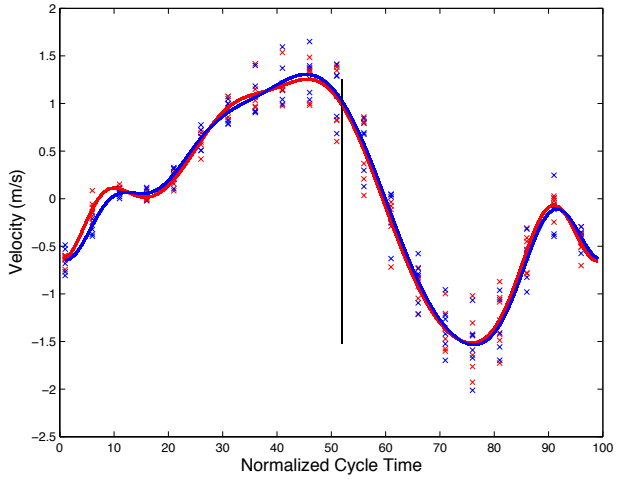

Figure 4.24: Velocity of the ankle for RFS (red) and nRFS (blue) conditions, toe off is indicated by vertical black line. Individual subject values are shown at each time point and indicated by a red and blue 'x' for RFS and nRFS conditions, respectively.

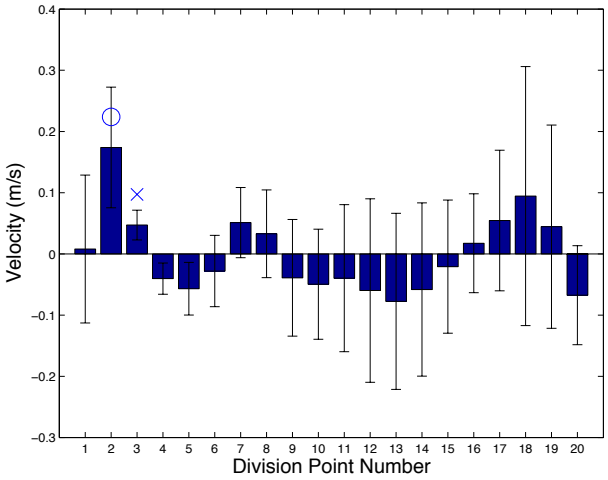

Figure 4.25: Differences (RFS-nRFS) in ankle velocity at 20 points on the average cycle. The average RFS value for all subjects at each point was subtracted from its corresponding value in the nRFS condition. Error bars represent the standard deviation of the differences. Significant differences between conditions are indicated by $*$ (p= 0.0025), $\times$ (p= 0.005) and $\circ$ (p= 0.01). Foot strike, toe off and the end of swing phase occurred at points 1, 11 and 20, respectively.

4.4 Ground reaction force

Ground reaction force was significantly greater following foot strike, at the time of the first peak, in the RFS condition (Figure 4.27). For the rest of stance, GRF was similar for both conditions. The GRF was normalized in cycles from foot strike to toe off and then the average GRF for each subject under both foot strike conditions, as well as the overall average for RFS and nRFS across all subjects. GRF shows a first impact peak during RFS, which is absent in nRFS condition. During the RFS trials, the first impact peak (Figure 4.26) occurred on average 27.7 ± 1.5 mS after foot strike.

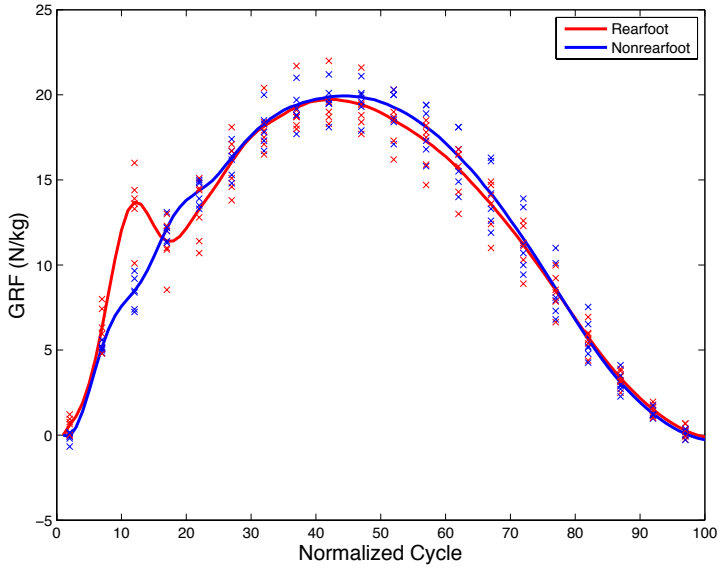

Figure 4.26: GRF averaged across all subjects under RFS (red) and nRFS (blue) conditions, toe off is indicated by vertical black line. Individual subject values are shown at each time point and indicated by a red and blue 'x' for RFS and nRFS conditions, respectively.

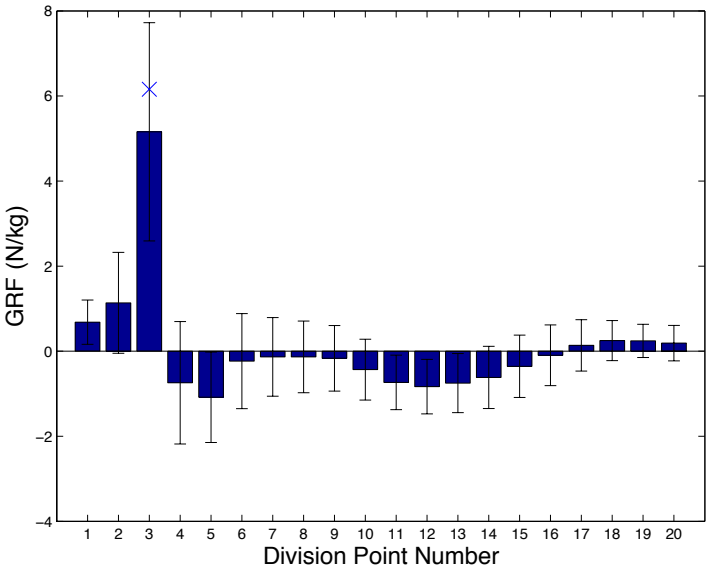

Figure 4.27: Differences (RFS-nRFS) in ground reaction force at 20 points on the average cycle. The average RFS value for all subjects at each point was subtracted from its corresponding value in the nRFS condition. Error bars represent the standard deviation of the differences. Significant differences between conditions are indicated by $*$ (p= 0.0025). Foot strike and toe off occurred at points 1 and 20, respectively.

4.5 Tibial acceleration

Tibial acceleration along the the anterior-posterior axis of the tibia, resultant acceleration and acceleration in the sagittal plane were significantly greater in the nRFS condition, indicated in Figure 4.28. The acceleration along the long axis of the tibia and and the medial-lateral axis did not show significant differences in foot strike conditions. The average peak acceleration was calculated for each subject under both foot strike conditions (Figure 4.29) and then averaged across all subjects for RFS and nRFS (Figure 4.30 and Table 4.4) . Five components of the acceleration were calculated and averaged: acceleration along the long axis of the tibia (A_x), anterior-posterior axis of the tibia (A_y) and the medial-lateral axis of the tibia (A_z). Additionally, the resultant acceleration (A_r) and acceleration along the vector in the A_xA_y direction were calculated and averaged.

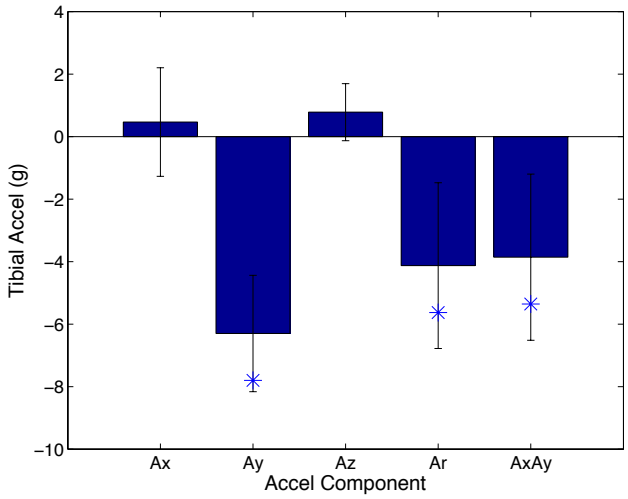

Figure 4.28: Differences (RFS-nRFS) in acceleration components (A_x, A_y, A_z, A_r, A_xA_y). The average RFS value for all subjects at each point was subtracted from its corresponding value in the nRFS condition. Error bars represent the standard deviation of the differences. Significant differences between conditions are indicated by $*$ (p= 0.05).

Table 4.4: Average peak acceleration components for RFS (red) and nRFS (red) conditions across all subjects.

Acceleration (g)					
FS Type	A_x	A_y	A_z	A_r	A_xA_y
Rearfoot	8.278 ± 2.642	5.688 ± 1.867	-3.138 ± 1.662	9.662 ± 2.971	9.547 ± 2.919
Nonrearfoot	7.813 ± 1.167	11.988 ± 1.835	-3.920 ± 1.314	13.790 ± 1.854	13.405 ± 1.929

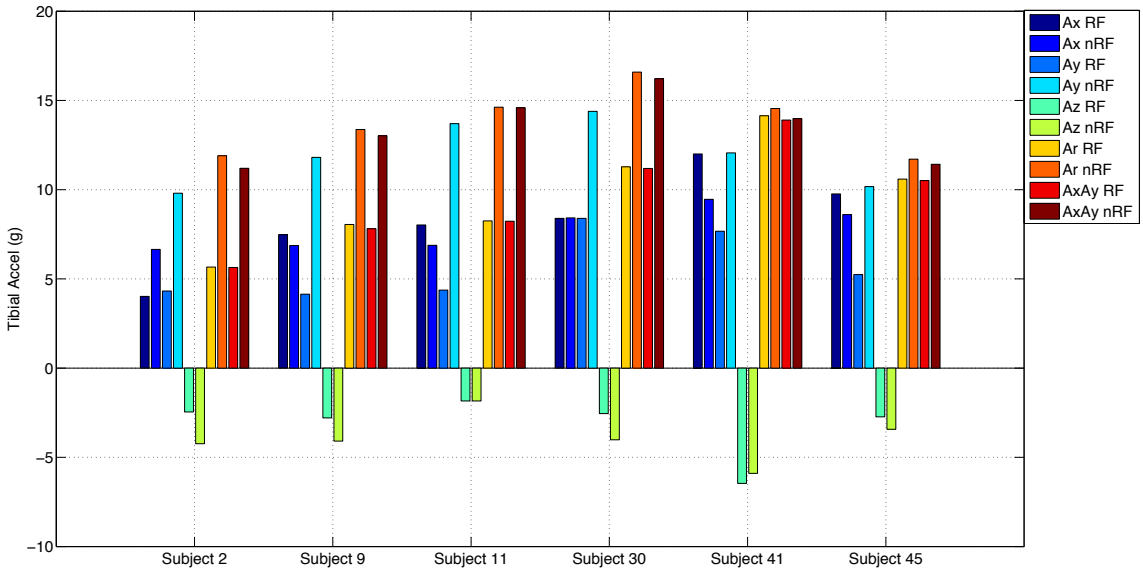

Figure 4.29: Tibial acceleration components for all subjects under RFS (red) and nRFS (blue) conditions. Components for each subject in the order A_x, A_y, A_z, A_r, A_xA_y, as indicated by the figure legend. Subjects 9 and 41 were habitual nRFS.

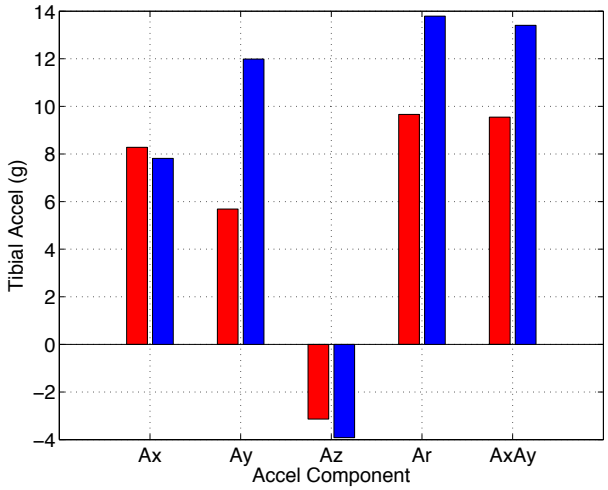

Figure 4.30: Tibial acceleration components A_x, A_y, A_z, A_r and A_xA_y averaged across all subjects under RFS (red) and nRFS (blue) conditions.

4.6 Electromyography

No significant differences were found in either the tibialis anterior or medial gastrocnemius muscle activation time or magnitude in the two conditions (Figure 4.32, 4.34). The EMG of

the medial gastrocnemius visually appeared to have an initial activation prior to foot strike (Figure 4.33), however due to high variability and a low number of subjects the difference observed was not statistically significant. Visually there did not appear to be any differences in the EMG activity for the tibialis anterior (Figure 4.31). EMG activity for the tibialis anterior and medial gastrocnemius was found for intervals ranging from 0.4 sec prior to foot strike to 0.4 seconds after foot strike and then normalized to 100 and averaged to find the average activation interval for each subject under both foot strike conditions. The average activation for both muscles across all subjects and under both foot strike conditions was then found.

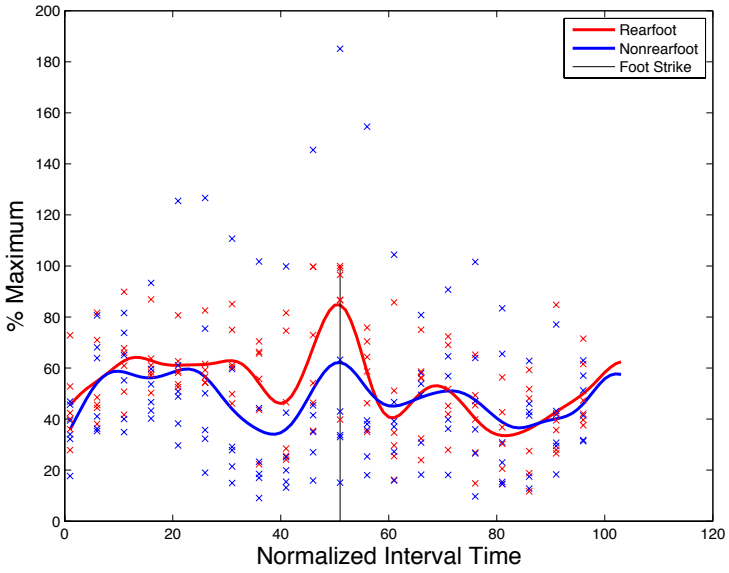

Figure 4.31: EMG of the tibialis anterior averaged across subjects under RFS (red) and nRFS (blue) conditions, toe off indicated by vertical black line. Individual subject values indicated by a red and blue 'x' for RFS and nRFS conditions, respectively.

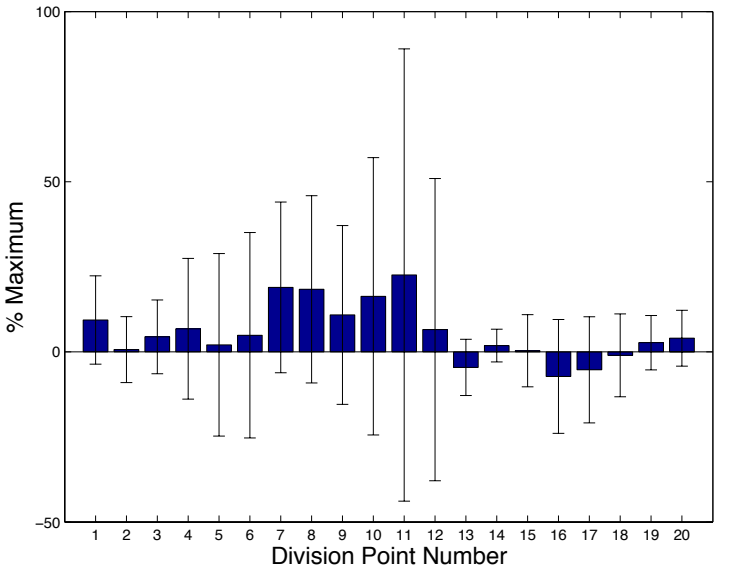

Figure 4.32: Differences (RFS-nRFS) in EMG of the tibialis anterior at 20 points on the average interval. The average RFS value for all subjects at each point was subtracted from its corresponding value in the nRFS condition. Error bars represent the standard deviation of the differences. No significant differences were found for muscle activity of the tibialis anterior between conditions. Foot strike occurred at point 11, with points 1 and 20 representing 0.4 s prior to and after foot strike, respectively.

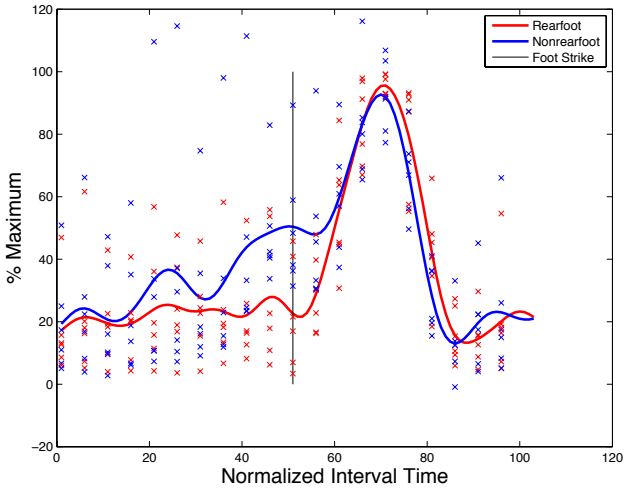

Figure 4.33: EMG of the medial gastrocnemius averaged across subjects under RFS (red) and nRFS (blue) conditions, toe off indicated by vertical black line. Individual subject values indicated by a red and blue 'x' for RFS and nRFS conditions, respectively.

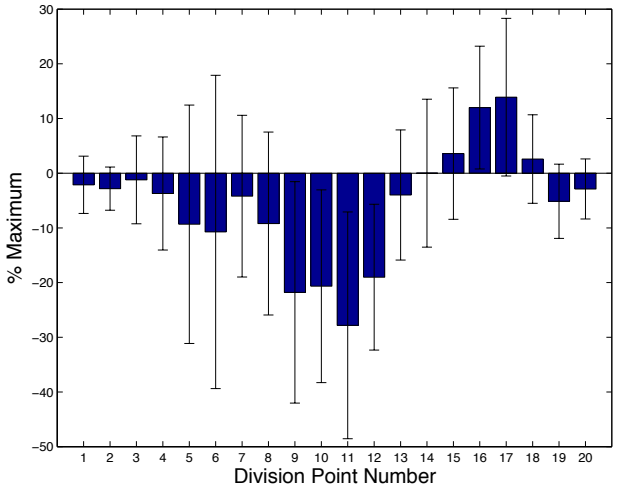

Figure 4.34: Differences (RFS-nRFS) in EMG of the medial gastrocnemius at 20 points on the average cycle. The average RFS value for all subjects at each point was subtracted from its corresponding value in the nRFS condition. Error bars represent the standard deviation of the differences. No significant differences were found for muscle activity of the medial gastrocnemius between conditions. Foot strike occurred at point 11, with points 1 and 20 representing 0.4 s prior to and after foot strike, respectively.

Chapter 5

Conclusion

5.1 Kinematics

Significant differences were found in rearfoot and nonrearfoot strike conditions for foot angle and ankle angle in the sagittal plane. This confirms previous research which has shown that running with a RFS pattern involves increased dorsiflexion at foot strike, thus an increase in foot and ankle angle. In contrast, running with a nRFS pattern results in a flat or plantar flexed foot at the time of foot strike, and thus a smaller foot and ankle angle when compared to RFS. There were no significant effects observed of foot strike pattern on frontal plane kinematics during running. However, there was greater variability between subjects in frontal plane kinematics (thigh and shank angles). This could be the result of individuals either pronating or supinating at foot strike, which would affect the variability of frontal plane angles as the ankle rolled toward or away from the mid-line, respectively.

Angle-angle diagrams of the thigh-knee and ankle-knee angle relationships revealed substantial differences in coordination between the two conditions. Half of the subjects showed decreased coordination at foot strike for the nRFS condition, where the thigh angle remained constant as the knee flexed. One subject had an overall decrease in coordination for the RFS condition, and two subjects did not present substantial differences in the thigh-knee angle diagrams. All of the subjects showed a substantial difference between RFS and nRFS conditions in the ankle-knee diagrams, indicating a difference in overall coordination between RFS and nRFS patterns. In the RFS condition, as the knee flexes at foot strike, the ankle dorsiflexes. In contrast, during nRFS the ankle plantar flexes while the knee is flexing. This difference in ankle kinematics results in the variation in ankle-knee diagrams between the conditions, and indicates an underlying overall difference in coordination.

5.2 Impact

5.2.1 Ground reaction force

Ground reaction force was similar for RFS and nRFS conditions, with the exception of the first peak present in the RFS pattern. The GRF was significantly greater in the RFS condition at the first peak, confirming the findings of previous studies that reported increased

initial impact in rearfoot runners. Following the impact peak, both conditions were similar in GRF magnitude for the remainder of stance. The initial impact peak in the GRF of rearfoot runners has been implicated by some in an overall increase in impact during running, and thus an increased risk of impact related injuries, such as stress fractures. Following that train of thought, the adoption of a forefoot striking pattern has recently been advocated by some as a means for overall reduction in the development of running related injuries. However, this theory should be investigated further, as there are many more factors at play during running in addition to an individual's ground reaction force.

5.2.2 Tibial acceleration

Tibial acceleration was significantly greater in the nonrearfoot strike condition for three of the five components. Acceleration in the anterior-posterior direction, acceleration in the sagittal plane and resultant acceleration (A_y, A_xA_y and A_r, respectively) all increased significantly during nRFS pattern running. Acceleration along the long axis of the tibia, as well as in the medial-lateral direction (A_x and A_z, respectively) were similar in nRFS and RFS conditions. This has implications in discussions of the benefits of different foot strike patterns. Despite an apparent reduction in impact during nRFS running which is seen in the GRF as a lack of the first impact peak, this does not translate into a reduction in the acceleration or shock that propagates up the tibia at foot strike. A significant increase in tibial acceleration in the anterior-posterior direction, seen in the nRFS condition, was likely due to the lack of plantar flexor control during nRFS. In the RFS condition the runner gradually decreases their acceleration in the anterior-posterior direction following foot strike through the controlled plantar flexion of the ankle. The large anterior-posterior tibial acceleration during nRFS running may contribute to an increase in bending moment and internal shear force in the tibia, thus exposing the runner to an increased risk of transverse fractures as failure on the tension side (anterior tibia) progresses transversely across the bone (posterior tibia). Thus, running with a nRFS pattern cannot be assumed to lead to an overall reduction in impact during running, and may even lead to increased risk of injury (such as tibial stress fractures) due to increased tibial acceleration.

5.2.3 Modified ankle moment

The calculation of modified ankle moment revealed a significant increase in ankle moment during running with a nRFS pattern. This may have implications in injury, as rate and magnitude of joint moments may cause repetitive stress damage in the connective and stabilizing tissues. The increase in loading rate at the ankle found in runners utilizing a nRFS pattern should be considered by individuals considering transitioning from a RFS to nRFS pattern, as this may result in injury during the acclimation period. However, due to the fact that the ankle moment reported in this study was "modified" because of lack of shear ground reaction force and center of pressure data, these findings should be verified when these data are available.

5.3 Electromyography

Muscle activation (EMG) of the tibialis anterior and medial gastrocnemius were not statistically different in RFS and nRFS conditions. This is surprising because of the different demands made on the plantar flexors during nonrearfoot running as indicated by the increased modified ankle moment and the altered kinematics. Visual examination of the mean medial gastrocnemius pattern shows the hypothesized pre-foot strike muscle activation in the nRFS condition, however this was not statistically significant due to the large EMG variability between subjects, as well as the small number of subjects tested. During nRFS running, the medial gastrocnemius activity should be greater due to the requirement that the plantor flexors absorb the load upon impact. The increase in muscle activity of the medial gastrocnemius during nRFS running, that was confirmed visually, may lead to increased muscle fatigue in individuals attempting to adpot a nRFS pattern. It then follows that there may be an increase in the potential for developing muscle overuse injuries as a result of muscle fatigue in individuals attempting to change their foot strike pattern whether it be the adoption of a nRFS or RFS pattern. The tibialis anterior did not show a visual difference in activity between conditions. This may be the result of the muscle being active at the same time in RFS and nRFS running, but performing a different function for each respective foot strike pattern. At foot strike in RFS running, the tibialis anterior is acting concentrically to dorsiflex the foot before and as the heel strikes, as well as acting eccentrically to control the rate of plantar flexion following foot strike. It was hypothesized that the tibialis anterior would not activate until later in stance during nRFS running, however it may be that the muscle is acting in coordination with the medial gastrocnemius during foot strike via dynamic coupling, or there may be "cross talk" into the tibialis anterior electrodes from the gastrocnemius muscle activity. Both observations of the expected pre-activation of the medial gastrocnemius and unexpected activation of the tibialis anterior during nRFS running should be verified through the testing of a greater number of subjects.

5.4 Study limitations

This study had some limitations which should be minimized in future studies examining the effects of foot strike pattern on kinematics, kinetics, tibial acceleration and muscle activation. Because of the exclusion of subjects who did not successfully change their foot strike pattern, the small subject population was a limitation. Future studies should test a larger number of individuals in order to minimize the effect of individual variability. Necessary sample size that would be required to determine significance was calculated (using Equation 5.1 [39]) for the EMG data of the medial gastrocnemius, as well as sample size requirements with different variance estimates, and these are shown in Table 5.1.

$$n = \frac{(t_{n-1,\alpha/2} + t_{n-1,\beta})^2}{d^2} \tag{5.1}$$

where

- n = sample size

- $t_{v,p}$ = the value from the Student's t-distribution with v degrees of freedom and p probability of a larger value
- α = probability of detecting a false effect
- $\beta = 1 - power$
- $power$ = probability of detecting a true effect
- $d = \delta/\sigma$
- δ = difference in population means
- σ = estimated standard deviation of paired response differences

Subjects had a very short time during which to acclimate to their modified foot strike pattern. This may have affected the ability for comparisons to be made between the two foot strike conditions, as some individuals were utilizing a modified strike pattern, and potentially had not fully adapted to their new way of running. Future studies should include a longer time for the adoption of a modified foot strike pattern in order to study the effects of foot strike pattern change on running biomechanics. Additionally, subjects could separated according to their habitual strike pattern and comparisons could be made between habitual strike patterns. Furthermore, EMG data are usually normalized to the maximum voluntary contraction muscle activity, which was not collected during this study. Instead, EMG data were normalized to the maximum muscle activation magnitude for each subject and each muscle during running with a RFS pattern. For the majority of subjects muscle activation magnitude was greatest in the RFS condition, however this may not have been the best approach for normalization since two of the subjects were running with a converted strike pattern in the RFS condition.

Another potential limitation of this study was the lack of data on shear ground reaction force and center of pressure, both needed for the calculation of ankle moments. Future studies should utilize a force platform that collects all components of GRF, as well as a pressure mat to track changes in center of pressure.

Table 5.1: Sample size (n) calculations based on data from the EMG of the medial gastrocnemius ($mean_{RFS} = 27.86$ % max, $mean_{nRFS} = 48.53$ % max, $\alpha = 0.05$, $power = 0.8$). The first value for the sample size calculation was done using the standard deviation from this study (17.67 % max). The calculation was also done for half the study standard deviation (8.84 % max), as well as various intermediate values.

Power Analysis	
Standard Deviation (% max)	Sample Size
17.67	12
15.46	9
13.25	7
11.05	5
8.84	3

5.5 Summary

In summary, findings in relation to the hypotheses were:

1. Activation of the medial gastrocnemius will be earlier and of greater magnitude during nonrearfoot striking as compared to rearfoot striking.
    - Hypothesis rejected
2. Nonrearfoot striking will result in two peaks in medial gastrocnemius muscle activity, the first corresponding to preparation for, and support of, initial contact and the second corresponding to propulsion during the stance phase.
    - Hypothesis rejected
3. Rearfoot striking will result in earlier and greater magnitude activation of the tibialis anterior muscle associated with the controlled dorsiflexion needed during foot strike.
    - Hypothesis rejected
4. Nonrearfoot striking will result in a larger resultant tibial acceleration.
    - Hypothesis accepted

This study found significant kinematic (ankle angle, foot angle and overall coordination) and kinetic (ground reaction force and resultant tibial acceleration) differences between runners utilizing a rearfoot strike pattern and those utilizing a nonrearfoot strike pattern. Hypothesized differences in the muscle activation of the tibialis anterior and medial gastrocnemius could not be verified due to a small number of subjects and variability in EMG data, and thus were rejected. Previously proposed benefits of the adoption of a nonrearfoot strike pattern during running require further examination as it was determined in this study that the use of a nonrearfoot strike pattern increases the resultant tibial acceleration, even with the absence of the impact peak in the ground reaction force present in the rearfoot strike pattern.

Bibliography

[1] A Altman and I Davis. Barefoot running: biomechanics and implications for running injuries. *Current Sports Medicine Reports*, 11(5):244–250, 2012.

[2] AR Altman and IS Davis. A kinematic method for footstrike pattern detection in barefoot and shod runners. *Gait and Posture*, 35(2):298–300, 2012.

[3] R Arendse, T Noakes, Azevedo, N Romanov, M Schwellnus, and G Fletcher. Reduced eccentric loading of the knee with the pose running method. *Medicine and Science in Sports and Exercise*, 36(2):272–277, 2004.

[4] E Arendt, J Agel, C Heikes, and H Griffiths. Stress injuries to bone in college athletes: a retrospective review of experience at a single institution. *The American Journal of Sports Medicine*, 31(6):959–968, 2003.

[5] E Arnold, S Hamner, A Seth, M Millard, and S Delp. How muscle fiber lengths and velocities affect muscle force generation as humans walk and run at different speeds. *The Journal of Experimental Biology*, 216(11):2150–2160, 2013.

[6] A Barr and M Barbe. Pathophysiological tissue changes associated with repetitive movement: a review of the evidence. *Physical Therapy*, 82(2):173–187, 2002.

[7] JM Bland and DG Altman. Multiple significance tests: the Bonferroni method. *The BMJ*, 310(170), 1995.

[8] M Bobbert, H Schamhardt, and B Nigg. Calculation of vertical ground reaction force estimates during running from positional data. *Journal of Biomechanics*, 24(12):1095–1105, 1991.

[9] E Boyer, B Rooney, and T Derrick. Rearfoot and midfoot/forefoot impacts in habitually shod runners. *Medicine and Science in Sports and Exercise*, 2013.

[10] P Cavanagh and P Komi. Electromechanical delay in human skeletal muscle under concentric and eccentric contractions. *European Journal of Applied Physiology and Occupational Physiology*, 42(3):159–163, 1979.

[11] P Cavanagh and M Lafortune. Ground reaction forces in distance running. *Journal of Biomechanics*, 13(5):397–406, 1980.

[12] R Cheung and I Davis. Landing pattern modification to improve patellofemoral pain in runners: a case series. *The Journal of Orthopaedic and Sports Physical Therapy*, 41(12):914–919, 2011.

[13] RTH Cheung and MJ Rainbow. Landing pattern and vertical loading rates during first attempt of barefoot running in habitual shod runners. *Human Movement Science*, 2014.

[14] H Crowell and I Davis. Gait retraining to reduce lower extremity loading in runners. *Clinical Biomechanics*, 26(1):78–83, 2011.

[15] A Daoud, G Geissler, F Wang, J Saretsky, Y Daoud, and D Lieberman. Foot strike and injury rates in endurance runners: a retrospective study. *Medicine and Science in Sports and Exercise*, 44(7):1325–1334, 2012.

[16] I Davis, C Milner, and J Hamill. Does increased loading rate lead to tibial stress fractures? a prospective study. *Medicine and Science in Sports and Exercise*, 36(5):S58, 2004.

[17] B De Wit, D De Clercq, and P Aerts. Biomechanical analysis of the stance phase during barefoot and shod running. *Journal of Biomechanics*, 33(3):269–278, 2000.

[18] A Diebal, R Gregory, C Alitz, and J Gerber. Forefoot running improves pain and disability associated with chronic exertional compartment syndrome. *The American Journal of Sports Medicine*, 40(5):1060–1067, 2012.

[19] W Edwards, J Gillette, J Thomas, and T Derrick. Internal femoral forces and moments during running: implications for stress fracture development. *Clinical Biomechanics*, 23(10):1269–1278, 2008.

[20] K Fields, J Sykes, K Walker, and J Jackson. Prevention of running injuries. *Current Sports Medicine Reports*, 9(3):176–182, 2010.

[21] EC Frederick. Kinematically mediated effects of sport shoe design: a review. *Journal of Sports Sciences*, 4:169–184, 1986.

[22] M Fredericson, F Jennings, C Beaulieu, and G Matheson. Stress fractures in athletes. *Topics in Magnetic Resonance Imaging*, 17(5):309–325, 2006.

[23] M Giandolini, P Arnal, G Millet, N Peyrot, P Samozino, B Dubois, and JB Morin. Impact reduction during running: efficiency of simple acute interventions in recreational runners. *European Journal of Applied Physiology*, 113(3):599–609, 2013.

[24] J Giuliani, B Masini, C Alitz, and B Owens. Barefoot-simulating footwear associated with metatarsal stress injury in 2 runners. *Orthopedics*, 34(7):e320–323, 2011.

[25] D Goss and M Gross. Relationships among self-reported shoe type, footstrike pattern, and injury incidence. *U.S. Army Medical Department Journal*, pages 25–30, 2012.

[26] D Goss and M Gross. A review of mechanics and injury trends among various running styles. *U.S. Army Medical Department Journal*, pages 62–71, 2012.

[27] A Gruber, B Umberger, R Miller, and J Hamill. The relationship between achilles tendon moment arm and running economy in rearfoot and forefoot runners. In *Official Journal of the American College of Sports Medicine, Indiana, USA, May 28-June 1, 2013*, volume 45, page S335, Indiana, USA, 2013. American College of Sports Medicine.

[28] CL Hamill, TE Clarke, EC Frederick, LJ Goodyear, and ET Howley. Effects of grade running on kinematics and impact force. *Medicine and Science in Sports and Exercise*, 16:185, 1984.

[29] A Hansen, D Childress, S Miff, S Gard, and K Mesplay. The human ankle during walking: implications for design of biomimetic ankle prostheses. *Journal of Biomechanics*, 37(10):1467–1474, 2004.

[30] H Hasegawa, T Yamauchi, and WJ Kraemer. Foot strike patterns of runners at the 15-km point during an elite-level half marathon. *Journal of Strength and Conditioning Research / National Strength & Conditioning Association*, 21:888–893, 2007.

[31] B Heiderscheit, E Chumanov, M Michalski, C Wille, and M Ryan. Effects of step rate manipulation on joint mechanics during running. *Medicine and Science in Sports and Exercise*, 43(2):296–302, 2011.

[32] A Hreljac. Impact and overuse injuries in runners. *Medicine and Science in Sports and Exercise*, 36(5):845–849, 2004.

[33] A Hreljac, R Marshall, and P Hume. Evaluation of lower extremity overuse injury potential in runners. *Medicine and Science in Sports and Exercise*, 32(9):1635–1641, 2000.

[34] E Joy and D Campbell. Stress fractures in the female athlete. *Current Sports Medicine Reports*, 4(6):323–328, 2005.

[35] M Lafortune. Three-dimensional acceleration of the tibia during walking and running. *Journal of Biomechanics*, 24, 1991.

[36] M Lafortune, P Cavanagh, H Sommer, and A Kalenak. Three-dimensional kinematics of the human knee during walking. *Journal of Biomechanics*, 25(4):347–357, 1992.

[37] CA Laughton, I Davis, and J Hamill. Effect of strike pattern and orthotic intervention on tibial shock during running. *Journal of Applied Biomechanics*, 19(2), 2003.

[38] D Lieberman, M Venkadesan, W Werbel, A Daoud, D'Andrea, S, I Davis, R Mang'eni, and Y Pitsiladis. Foot strike patterns and collision forces in habitually barefoot versus shod runners. *Nature*, 463(7280):531–535, 2010.

[39] StatsDirect Limited. *Sample size for paired t test*, 2000 (accessed July 28, 2014).

[40] B Marti, J Vader, C Minder, and T Abelin. On the epidemiology of running injuries the 1984 bern grand-prix study. *The American Journal of Sports Medicine*, 16(3):285–294, 1988.

[41] GO Matheson, DB Clement, DC McKenzie, JE Taunton, DR Lloyd-Smith, and JG MacIntyre. Stress fractures in athletes. a study of 320 cases. *American Journal of Sports Medicine*, 15(1):46–58, 1987.

[42] AM McBryde. Stress fractures in runners. *American Journal of Sports Medicine*, 4(4):737–752, 1985.

[43] TA McMahon, G Valiant, and EC Frederick. Groucho running. *Journal of Applied Physiology*, 62:2326–2337, 1987.

[44] C Milner, R Ferber, C Pollard, J Hamill, and I Davis. Biomechanical factors associated with tibial stress fracture in female runners. *Medicine and Science in Sports and Exercise*, 38(2):323–328, 2006.

[45] C Munro, D Miller, and A Fuglevand. Ground reaction forces in running: a reexamination. *Journal of Biomechanics*, 20(2):147–155, 1987.

[46] B Nigg. The role of impact forces and foot pronation: a new paradigm. *Clinical Journal of Sports Medicine*, 11:2–9, 2001.

[47] B Nigg and J Wakeling. Impact forces and muscle tuning: a new paradigm. *Exercise and Sport Sciences Reviews*, 29(1):37–41, 2001.

[48] E Olin and G Gutierrez. EMG and tibial shock upon the first attempt at barefoot running. *Human Movement Science*, 32(2):343–352, 2013.

[49] M Pohl, D Mullineaux, C Milner, J Hamill, and I Davis. Biomechanical predictors of retrospective tibial stress fractures in runners. *Journal of Biomechanics*, 41(6):1160–1165, 2008.

[50] S Ridge, A Johnson, U Mitchell, I Hunter, E Robinson, B Rich, and S Brown. Foot bone marrow edema after a 10-wk transition to minimalist running shoes. *Medicine and Science in Sports and Exercise*, 45(7):1363–1368, 2013.

[51] B Rooney and T Derrick. Joint contact loading in forefoot and rearfoot strike patterns during running. *Journal of Biomechanics*, 46(13):2201–2206, 2013.

[52] CE Rothschild. Primitive running: a survey analysis of runners' interest, participation, and implementation. *Journal of Strength and Conditioning Research*, 45(7):1363–1368, 2012.

[53] S Sasimontonkul, B Bay, and M Pavol. Bone contact forces on the distal tibia during the stance phase of running. *Journal of Biomechanics*, 40(15):3503–3509, 2007.

[54] A Schinkel-Ivy, T Burkhart, and D Andrews. Leg tissue mass composition affects tibial acceleration response following impact. *Journal of Applied Biomechanics*, 28(1):29–40, 2012.

[55] R Seeley, P Tate, and T Stephens. Muscular system: Gross anatomy. In *Anatomy and Physiology*. McGraw-Hill, Texas, 2005.

[56] R Seeley, P Tate, and T Stephens. Muscular system: Histology and physiology. In *Anatomy and Physiology*. McGraw-Hill, Texas, 2005.

[57] Y Shih, K Lin, and T Shiang. Is the foot striking pattern more important than barefoot or shod conditions in running? *Gait and Posture*, 38(3):490–494, 2013.

[58] M Shorten and MIV Mientjes. The heel impact force peak during running is neither heel nor impact and does not quantify shoe cushioning effects. *Footwear Science*, 3, 2011.

[59] M Shorten and D Winslow. Spectral analysis of impact shock during running. *International Journal of Sport Biomechanics*, 8(4), 1992.

[60] EB Simonsen, T Alkjaer, and PC Raffalt. Reflex response and control of the human soleus and gastrocnemius muscles during walking and running at increasing velocity. *Experimental Brain Research*, 219(2):163–174, 2012.

[61] R Squadrone and C Gallozzi. Biomechanical and physiological comparison of barefoot and two shod conditions in experienced barefoot runners. *Journal of Sports Medicine and Physical Fitness*, 49(1):6–13, 2009.

[62] J Taunton, M Ryan, D Clement, McKenzie, D, Lloyd-Smith, D, and B Zumbo. A retrospective case-control analysis of 2002 running injuries. *British Journal of Sports Medicine*, 36(2):95–9101, 2002.

[63] J Tweed and M Barnes. Is eccentric muscle contraction a significant factor in the development of chronic anterior compartment syndrome? a review of the literature. *The Foot (Edinburgh, Scotland)*, 18(3):165–170, 2008.

[64] R van Gent, D Siem, M van Middelkoop, A van Os, Bierma-Zeinstra, S, and B Koes. Incidence and determinants of lower extremity running injuries in long distance runners: a systematic review. *British Journal of Sports Medicine*, 41(8):469–80; discussion 480, 2007.

[65] V von Tscharner, B Goepfert, and B Nigg. Changes in EMG signals for the muscle tibialis anterior while running barefoot or with shoes resolved by non-linearly scaled wavelets. *Journal of Biomechanics*, 36(8):1169–1176, 2003.

[66] J Wakeling, V Von Tscharner, B Nigg, and P Stergiou. Muscle activity in the leg is tuned in response to ground reaction forces. *Journal of Applied Physiology*, 91(3):1307–1317, 2001.

[67] B Warr, R Fellin, P Frykman, S Sauer, D Gross, and J Seay. No differences in self-reported injuries or performance between characterized foot-strike patterns amongst us army soldiers. In *Official Journal of the American College of Sports Medicine, Indiana, USA, May 28-June 1, 2013*, volume 45, page S333, Indiana, USA, 2013. American College of Sports Medicine.

[68] D Williams, D Green, and B Wurzinger. Changes in lower extremity movement and power absorption during forefoot striking and barefoot running. *International Journal of Sports Physical Therapy*, 7(5):525–532, 2012.

[69] DS Williams, IS McClay, and KT Manal. Lower extremity mechanics in runners with a converted forefoot strike pattern. *Journal of Applied Biomechanics*, 16(2):210–218, 2000.

[70] R Willy and I Davis. Kinematic and kinetic comparison of running in standard and minimalist shoes. *Medicine and Science in Sports and Exercise*, 46(2):318–323, 2014.